Biomass and Bioenergy 194 (2025) 107635

Contents lists available at ScienceDirect

Biomass and Bioenergy

journal homepage: www.elsevier.com/locate/biombioe

Hydrothermal liquefaction of *Caulerpa sertularioides*: Optimized biocrude production and characterization with pretreatment techniques

Ziba Borazjani [a], Reza Azin [b,*], Shahriar Osfouri [a], Rahim Karami [c], Eric Kennedy [c], Michael Stockenhuber [c]

[a] Department of Chemical Engineering, Faculty of Petroleum, Gas, and Petrochemical Engineering, Persian Gulf University, Bushehr, Iran
[b] Department of Petroleum Engineering, Faculty of Petroleum, Gas, and Petrochemical Engineering, Persian Gulf University, Bushehr, Iran
[c] School of Engineering, University of Newcastle, NSW, 2308, Australia

ARTICLE INFO

Keywords:
Biocrude
Optimization
Macroalgae
Pretreatment

ABSTRACT

Hydrothermal liquefaction (HTL) is presented as an eco-friendly method for producing biocrude from algal biomass, specifically macroalgae, which are abundant resources but often overlooked for biofuel production. This research aimed to create sustainable fuel from macroalgae and explored HTL product yields alongside ultrasonic and microwave pretreatments. Focusing on the green macroalga *Caulerpa sertularioides* in a batch reactor, the study used response surface methodology to analyze operational parameters like temperature (250–350 °C), pressure (50–150 bar), and feedstock concentration (3–10 wt%). Optimal conditions were identified at 350 °C, 150 bar, and 9.75 wt% feed concentration, achieving a biocrude yield of 22.15 wt%. The biocrude showed a high heating value of 39.17 MJ/kg with energy recovery at 73.19 %. Predominantly consisting of complex cyclic compounds such as acids and ketones, about 35.79 % of biocrude components have boiling points similar to standard diesel oil. However, an upgrading process is necessary due to the high oxygen content. Pretreatment using microwave and ultrasonication at 350 °C did not enhance biocrude yield.

1. Introduction

An increase in environmental awareness leads to a considerable transition in research focus towards the use of more sustainable and renewable energy sources. Biomass conversion to biofuels technologies have attracted much attention due to their potential to integrate into pre-existing infrastructure [1]. Hydrothermal liquefaction (HTL) stands out as one of the most effective techniques for biomass processing and has emerged as a highly promising technology for future applications. HTL converts biomass into four phases, notably solid residue, gas phase and aqueous products, and biocrude [2] produced at high temperatures (200–500 °C) and pressures (5–30 MPa) [3]. The primary product derived from HTL is a biocrude oil, which exhibits an energy density typically between 30 and 40 MJ/kg [4,5]. One of the primary benefits of HTL lies in its ability to process biomass in its high water content state, thereby decreasing the substantial energy demands typically associated with drying biomass. Therefore, HTL has emerged as a particularly advantageous process for converting biomass with high moisture content, including algae [6].

HTL variables include reaction temperature and pressure, solid and liquid residence time, feed concentration, presence of a solvent and/or catalyst, and heating rate [7]. Temperature stands as a critical operational variable in the HTL process, significantly influencing both the yield and the characteristics of the biocrude by changing water properties [8,9]. Typically, a rise in temperature acts as a catalyst for the breakdown of organic matter, subsequently improving both the quantity and the quality of the products [10]. Elevated temperatures, beyond a certain threshold, lead to an increase in the yield of solid and gas phases, while concurrently diminishing both the quantity and the quality of the biocrude [11]. The optimum temperature of algal HTL is suggested to be between 300 and 350 °C, which depends on the biochemical component of algae [7,12,13]. For instance, Eboibi et al. [14] achieved the highest biocrude yield of 58 % and 42 wt% from *Tetraselmis* sp. and *Spirulina* sp. at 350 °C. Their results indicated that the increase in temperature also had positive effects on the heating value and the extent of carbon and nitrogen recovery. Zhou et al. [15] obtained the highest product yield at a temperature of 300 °C in which biocrude was produced with a maximum yield of 23.4 wt% from *Enteromorpha prolifera*. Recently, HTL

* Corresponding author.
E-mail address: reza.azin@pgu.ac.ir (R. Azin).

https://doi.org/10.1016/j.biombioe.2025.107635
Received 27 October 2024; Received in revised form 8 December 2024; Accepted 17 January 2025
Available online 24 January 2025

of microalgae grown in wastewater was performed by Arun et al. [16]. Results indicated that the highest biocrude yield was 29.37 wt% at 300 °C. Fernandes et al. [17] showed that the maximum biocrude production of 5.25 wt% is obtained from HTL of the red macroalga *Gracilaria corticata* at 350 °C. The optimum reaction time is significantly influenced by the biomass variety and the temperature, with adjustments made to optimize biocrude production yields [18,19]. Prolonging the reaction time typically increases the conversion of biomass material [20]. However, an increase in the conversion rate does not necessarily correlate with improved biocrude yields. The determination of an ideal reaction time is intricately linked to a range of other factors [8]. Previous studies have indicated that both short and long retention times, when coupled with varying reaction temperatures, result in biocrude with disparate yields and characteristics [21]. Typically, maximal biocrude production is achieved when algae are subjected to an optimal residence time of 30 min [22–24]. For instance, Li et al. [25] found that the highest biocrude yield of 43.8 wt% was produced through HTL of *Ulva* macroalgae in 30 min. The result was similar to the results presented by Liu et al. [24] which a maximum biocrude of 43.6 wt% was achieved in HTL of *Spirulina* microalgae in 30 min. The optimization of the ratio of biomass to solvent is crucial in influencing the yield of products in the HTL process. Research indicates that the feed concentration typically ranges from 10 % to 20 %, with many studies specifically identifying 10 wt% as the optimal concentration [22]. For instance, the greatest bio-oil yields recorded were 47.5 wt% from *Nannochloropsis* and 32.5 wt% from *Chlorella* under HTL conditions of 10 wt % algal concentration, a temperature of 300 °C, and a duration of 30 min [26]. *Cyanobacteria* sp. yielded a maximum of 21.10 wt% bio-oil when processed at a feed concentration of 10 wt%, a temperature of 325 °C, and a time frame of 45 min [27]. Typically, a high increase in feed concentration results in lower biocrude yields while leading to higher amounts of solid residue and gas [22]. The decline in biocrude yield is attributed to factors such as re-polymerization reactions, intermolecular forces, and the solubility of compounds [28]. In analyzing the impact of pressure within both continuous and batch operations, it is typically considered dependently alongside temperature as a variable. In the HTL process, pressure does not affect the properties of the solvent; rather, it is effective in influencing properties such as gas dissolution which in turn affects the biomass decomposition reactions [29]. To explore the effect of varying pressure of the reaction, methodologies such as the injection of gas [30] or modification of the reactor's volume are utilized [31]. Remón et al. [8] found that in catalytic HTL at long residence times, performing the process at a pressure of 120 bar compared to 50 bar led to an increase in biocrude yield. Mathanker et al. [30] indicated that the optimal production of heavy oil, reaching a peak at 29.25 wt%, was achieved when the temperature was maintained at 300 °C and the pressure was sustained at approximately 152 bar. However, further pressure increases reduce the biocrude yield due to operating out of the optimal condition of the pressure-temperature range [32].

While the HTL technique offers several advantages over alternative biofuel synthesis methodologies, it is not without its challenges. One significant limitation is the elevated levels of nitrogen and oxygen atoms present within the biocrude. This issue can lead to a decrease in the higher heating value (HHV), potentially compromise catalyst effectiveness through poisoning, and contribute to an increase in the fluid's viscosity [23]. Implementing a pretreatment strategy prior to HTL can result in the production of biocrude containing a low nitrogen and oxygen content [33]. To facilitate the extraction of vital components for biocrude production, it is imperative to disrupt the cell wall, which serves as a barrier safeguarding the components within the cellular membrane. This disruption acts as a preliminary step in the pretreatment phase, enabling access to the crucial intracellular constituents [34]. Two effective pretreatment processes include ultrasonication and the use of microwave radiation. The disruption of algal cells can be achieved through the application of ultrasonic vibrations, generally utilizing an energy output ranging from 100 to 200 W over a period spanning 5–10 min [35,36]. Table S1 presents the studies on the ultrasonic pretreatment of algae. The effect of using ultrasonication as a pretreatment method was reported for several algae. In some cases, ultrasonication increased the yield [37,38], and in others, the ultrasonic pretreatment did not affect the performance in the HTL of microalgae [39–41]. Also, some studies show that ultrasonic pretreatment increases the yield of compounds of lower boiling point in the biocrude [40,42]. In a study conducted by Saber et al. [43], it was observed that the application of ultrasonic pretreatment during the HTL process resulted in an increase in biocrude production with a reduced oxygen content, which in turn contributed to an elevation in the calorific value of the resulting fuel. Conversely, research by Kapusta showed that the influence of ultrasound on the biocrude composition was negligible [44]. Garoma et al. [37] and Heo et al. [38] showed that ultrasonication increased biocrude yield. However, Hu et al. [39] and Halim [40] reported that ultrasonic pretreatment did not affect the performance of cell disruption of microalgae. Although ultrasonic pretreatment has its advantages in terms of scalability and reduced operational expenditure, the result of ultrasonic pretreatment highly depends on feedstock and operating conditions [22]. Compared to conventional HTL, utilizing microwave irradiation as a preliminary step has been demonstrated to increase the biocrude yield [45]. When the microwave irradiates the cell inside, oscillation of polar compounds causes rapid heating, which leads to cell rupture and improves the performance of the extraction [35]. Several researchers have employed the technique of microwave pretreatment (Pre-M) to obtain high-yield biofuels. An overview of recent studies on the pretreatment microwave process is summarized in Table S2. In their research, Ma et al. [35] demonstrated that microwave-assisted extraction of lipids was more efficient and rapid than using an ultrasonic pretreatment technique. Similarly, Lee et al. [46] conducted comparative analyses on several pretreatment methods, including sonication, microwaving, bead-beating, autoclaving, and the employment of a 10 % NaCl solution. Their findings indicated that microwave-assisted technology stood out as the most proficient and straightforward method for the extraction of lipids from microalgae. Onumaegbu et al. [47] and Biller et al. [48] also employed microwave pretreatment in their studies and validated the results reported by Lee et al. [46]. Table S2 showed that Pre-M-HTL took place at a temperature of 140-100 °C for less than 12 min.

The most promising raw material for biofuel production is macro- and micro-algae. Despite the higher lipid content of microalgae, the high cost of harvesting microalgae and the need for large-scale cultivation are challenges in biocrude production. Also, the potential of microalgae produced in low-efficiency, costly photobioreactors for producing value-added products limits their use for biocrude production [49]. Although macroalgae have limited use in industry, they can be harvested rather easily and display a higher growth rate. Consequently, they present a suitable alternative source as a renewable feedstock for the generation of biofuels [50]. Aquatic plants, especially seaweed or macroalgae, can be considered abundant and available sources for bioenergy production. Also, macroalgae with their high biodiversity in marine water have one of the best benefits for efficient water consumption. The Persian gulf coasts have a good potential for algae cultivation and easy implementation of large-scale growth ponds because of the good humidity, long-term irradiation, and significant CO_2 production by power plants, gas plants, and petrochemical complexes in this area [51]. Few studies performed to evaluate the potential of macroalgae to produce biofuel through HTL. Typically, macroscopic algal species are characterized by a relatively low lipid concentration, often comprising less than 5 % of their dry mass [52,53]. The emphasis on lipid composition underscores the potential of macroalgae as a valuable source for the generation of oil-derived bioproducts [54]. Also, the availability and abundance of macroalgae are key factors in selecting the most suitable macroalgae for biocrude production. The reported ranges of the lipid content of green algae *Caulerpa sertularioides* were 0.92–9.13 wt% [55–59], which is widespread, in in which macroalgae that could be observed in offshore

platforms and coastal areas. Also, they can be cultivated in artificial ponds. Moreover, no study was found to produce biocrude by HTL of *Caulerpa*. Hence, *Caulerpa* macroalgae has the potential to be a beneficial choice for biocrude production due to its lipid content and widespread availability.

To the best of our knowledge, there is no study on the production of biofuels by HTL from the green algae *Caulerpa*; thus, there is a lack of information, knowledge, and insight into the challenges associated with this alga when selected as the feed for HTL. The literature review indicated that little attention was paid to the pressure effect on HTL product yield obtained from algae [30,60,61]. No study was found which evaluated the influence of temperature, pressure, and feed concentration on biocrude production through HTL. Also, Pre-M-HTL studies are limited, and less attention has been paid to the effect of microwave power as a pretreatment of algae. Besides, the effect of the pretreatment heating method depends on the characteristics and nature of the raw material utilized. Hence, there is a knowledge gap with respect to the use of microwave or ultrasonic as pretreatment of HTL. The main aims of this study included an evaluation of the quality and quantity of biocrude produced through the HTL process from selected macroalgae, with changes in critical variables such as temperature, pressure, and feedstock concentration, which have complex effects on each other, and the examination of influence of power input on pretreatment on the biocrude yield. This study is novel in three ways: (1) for the first time, the effect of pressure was examined with a change in HTL temperature and algae slurry in the reactor simultaneously, while this method has not been previously reported, (2) HTL operating parameters including temperature, pressure, and feedstock concentration, were optimized based on the quantitative approach for modeling and analyzing the relationships between multiple variables, and (3) the ultrasonic- and microwave-pretreatment of HTL and understanding its performance from the marine feedstock were evaluated. The experimental design was performed based on response surface methodology (RSM) [62,63]. The quality of biocrude was evaluated by various analyses such as CHN, Fourier transforms infrared (FT-IR), thermal gravimetric analysis (TGA), and gas chromatography-mass spectroscopy (GC-MS). Moreover, the characterization of the HTL byproducts was carried out to evaluate their reuse possibility. Besides, the quantity of each product was evaluated by measuring the yield of the product. Finally, a comparison was made between autoclave-assisted HTL and microwave and ultrasonic pretreatment HTL of selected algae.

2. Materials and method

2.1. Materials and apparatus

Caulerpa sertularioides macroalgae was collected from the north coast of the Persian Gulf, Bushehr, Iran (28°50′N, 50°51′E). In addition, distilled water was used to prepare the algae slurry. Nitrogen gas was utilized to purge air in the HTL reactor. Moreover, dichloromethane (DCM), sourced from Merck Chem. Co., used as an extraction solvent to separate the biocrude from the aqueous phase. Also, high-quality filter papers from Whatman, England, were utilized to separate the remaining solid residue. The algae were ground to a fine powder using a planetary ball mill to increase the surface area of the algae. The milling process involved mixing dried algae with metal balls in a specific mass ratio of 1–10 and ground for 2 h. This reactor, made of stainless steel and capable of holding 100 mL, was custom-designed to withstand temperatures up to 400 °C and pressures as high as 25 MPa.

2.2. Hydrothermal liquefaction

The HTL process includes liquefaction, filtration, and extraction. Fig. 1 shows a procedure for producing HTL products. First, a composition was formulated by combining specific proportions of algae biomass with water to achieve a weight ratio (3–10 wt% biomass). Second, the slurry was placed inside the autoclave reactor for the HTL process. To maintain an inert environment free from air, nitrogen gas was introduced into the HTL reactor. The reactor was equipped with a heater, and the reaction time was recorded when the temperature of the slurry reached the designed pressure and temperature. The autoclave remained at a constant temperature and pressure for 30 min. The filled volume of the reactor vessel was changed to reach the desired pressure [31]. The time was recorded from the moment that the reactor temperature and pressure remained constant. At the end of the reaction, the reactor was subsequently cooled to the ambient temperature. Subsequently, the gaseous products were released via a valve to equalize the pressure inside the reactor to approximately ambient pressure. Then, DCM was added as an extraction solvent to the reaction medium vessel. This was followed by the process of liquid-solid separation, where the mixture was passed through the filter paper to separate any residual particulate matter. The solid phase was separated from the liquid products by vacuum filtration and dried at 105 °C for 24 h, then weighed

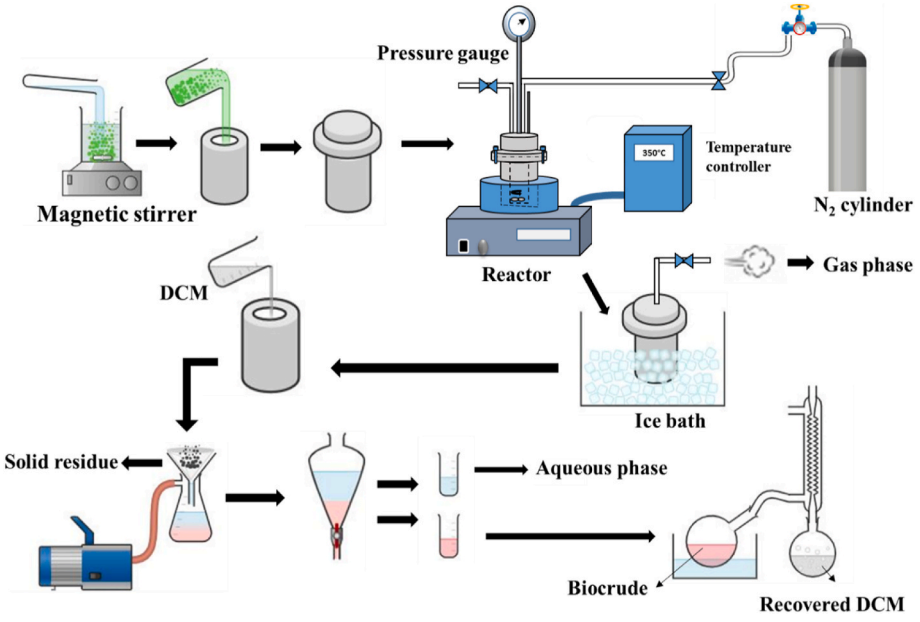

Fig. 1. Schematic procedure of the HTL process.

as solid residue [64]. The liquid was maintained within a two-phase separating funnel for 24 h. Separation of DCM-soluble and aqueous phases was done by gravity force in the separating funnel.

The DCM-soluble material was placed in a rotary evaporator at 45 °C for 15 min [65] to recover DCM, then put in a vacuum oven to evaporate the remaining DCM at 35 °C and 10 kPa for 5 min [66]. Finally, a dark liquid (biocrude) product was obtained. The aqueous phase was placed in a drying oven at 60 °C to evaporate the water completely over 3 days [67]. The aqueous phase yield accounted for the mass of dissolved aqueous constituents remaining after DCM extraction, filtration, and water evaporation [68].

2.3. Product yields, HHV, and ER calculation

The HTL product yield was calculated by dividing the amount of dry algae, while the gas yield was based on mass balance estimations. Mass yield and energy recovery were used to analyze the experimental results. The mass yields of different products (biocrude, solid residue, aqueous phase, and gas) were calculated as follows (Eqs. (1)–(4)) [42].

$$Y_{BC} = \frac{W_{BC}}{W_{DA}} \times 100 \quad (1)$$

$$Y_{SR} = \frac{W_{S}}{W_{DA}} \times 100 \quad (2)$$

$$Y_{AP} = \frac{W_{AP}}{W_{DA}} \times 100 \quad (3)$$

$$Y_{G} = 100 - (Y_{BC} + Y_{SR} + Y_{AP}) \quad (4)$$

where Y_{BC}, Y_{SR}, Y_{AP} and Y_{G} are the mass yield of biocrude, solid residue, aqueous phase, and gas, respectively. Also, W_{BC} , W_{S}, W_{AP}, and W_{DA} indicate the weight of biocrude, solid, aqueous phase, and dry algae. Moreover, the HHV of HTL products was calculated by the calorimetry empirical correlation of Eq. (5) [69]. Also, Eq. (6) was used to estimate the energy recovery (ER) of products from HTL of algae.

$$HHV\ (MJ/kg) = 0.3491 \times C + 1.1783 \times H + 0.1005 \times S - 0.1034 \times O - 0.0151 \times N - 0.0211 \times Ash \quad (5)$$

$$ER = \frac{HHV_{BC}}{HHV_{DA}} \times Y_{BC} \times 100 \quad (6)$$

where C, H, N, S, O, and Ash represent carbon, hydrogen, nitrogen, oxygen, sulfur, and ash based on the moisture-free weight. HHV_{BC} and HHV_{DA} are the high heating value of biocrude and algae. The effects of temperature, pressure, and feed concentration were considered in this study to examine the potential of biocrude production from green macroalgae. A reaction time of 30 min was chosen for HTL of *Caulerpa sertularioides* macroalgae based on the repeatable optimal time found in the literature [11,70,71].

2.4. Experimental design

he experimental design was performed using RSM. The RSM serves as a quantitative approach for modeling and analyzing the relationships between multiple variables. In particular, the central composite design (CCD) stands out as an optimal strategy within RSM for examining the influences of varying parameters [63]. Analysis of variance (ANOVA) was used to analyze HTL product yields. Data derived from the proposed experimental investigations were quantitatively analyzed and subsequently modeled using a polynomial regression equation, as shown in Eq. (7) [72].

$$Y = \beta_0 + \sum_{i=1}^{k} \beta_i X_i + \sum_{i=1}^{k} \beta_{ii} X_i^2 + \sum_{i=1}^{k-1} \sum_{j>i}^{k} \beta_{ij} X_i X_j \quad (7)$$

where Y and X are the predicted response and the amount of the investigated factor, respectively. β_0 is the constant coefficient, β_i is the linear coefficient, β_{ii} is the quadratic coefficient, and β_{ij} is the interaction coefficient. In this study, a standard CCD with three variables, i.e. temperature, pressure, and feed concentration was used to examine HTL product yields. The factors and levels are given in Table 1. The RSM design suggests 17 tests and includes 6 axial points, 8 cubic points, and 1 center point with 3 repeats for the central point. The range of variables was 250–350 °C for temperature, 50–150 bar for pressure, and 3–10 wt % for biomass concentration. The Design-Expert software version 13 was employed to analysis the experimental results.

2.5. Algae and products characterization

The biochemical component of the biomass has a direct effect on the quantity and quality of the HTL products. In general, the composition of algae includes lipids, proteins, carbohydrates, moisture, and ash. The lipid content is the main composition of biomass for biofuel production [73,74]. The lipid content was determined by Soxhlet extraction. The Kjeldahl method was also used to estimate the protein content of algae [75,76]. One gram of algae powder was weighed and then placed in the oven for 24 h at a temperature of 100 °C to estimate the moisture content of the algae. The moisture content was calculated according to the weight difference between dried powder and fresh sample Eq. (8) [10]. The ash proportion was quantified by contrasting the mass of the sample post-incineration with its pre-incineration mass. In this way, some algae powder was weighed and placed in the furnace at a temperature of 550 °C for 5 h [77]. Carbohydrate content was calculated by a balance of other constituents using Eq. (9) [78].

$$\%W_{Moisture} = \frac{W_{Dried\ powder} - W_{Fresh\ sample}}{W_{Fresh\ sample}} \times 100 \quad (8)$$

$$X_{Car} = 100 - (X_{Lip} + X_{Pro} + X_{Ash}) \quad (9)$$

where $\%W_{Moisture}$ is the percentage of moisture fraction of algae. $W_{Dried\ powder}$ and $W_{Fresh\ sample}$ are algae weight in dried and fresh condition. X is the mass fraction (wt%) of each biochemical component such as lipid, protein, ash, and carbohydrate in Eq. (9). C H N, O elemental analysis was used to determine elements of feed, biocrude, and solid

Table 1
Levels of operation parameters in experiment design.

Experimental variables	Symbol	Coded level of variables				
		−1.682	−1	0	1	1.682
Temperature (°C)	A	215.91	250	300	350	384.09
Pressure (bar)	B	15.91	50	100	150	184.09
Feed concentration (wt %)	C	0.61	3	6.5	10	12.38

phase [76]. The amount of oxygen element (O) was determined by a balance of other elements using Eq. (10) [79].

$$O = 100 - (C + H + N + S + Ash) \quad (10)$$

GC-MS and GC were used to identify the biocrude and gaseous compounds, respectively [66,80]. TGA was performed to examine changes in the weight of the biocrude with increasing temperature and the boiling point of biocrude compounds. The process of increasing temperature was done at a rate of 10 °C per minute, and the process of changing the weight of the biocrude with increasing temperature was recorded and analyzed from the ambient temperature to the temperature of 900 °C [10]. The FT-IR of biocrude was performed using a model FT-IR 4600 spectrometer equipped with a KBr plate beam splitter to determine the main organic components based on the peaks of the functional groups [76,81]. Brunauer-Emmett-Teller (BET) analysis was employed to ascertain key physical characteristics of materials, including their specific surface area, pore volume, average pore diameter, and distribution of pore sizes. Total organic carbon (TOC) was calculated with a TOC analyzer. The amount of total nitrogen was calculated by the Kjeldahl method [75]. The amount of chemical oxygen demand (COD) of the aqueous phase was determined with the COD HACH device. In addition, the total dissolved solids (TDS) and pH were calculated by TDS analysis and a pH meter.

2.6. Pretreatment method

A comparative study of the microwave and ultrasonication conditions can help evaluate the pretreatment effect on the HTL of *Caulerpa sertularioides* algae. Algal slurries were processed by microwave with a volume capacity of 800 ml and designed to a maximum temperature of 190 °C and a maximum power of 1400 W. Moreover, the ultrasonic homogenizer was used with a maximum temperature of 120 °C and a maximum power of 200 W. Literature analysis showed that the operating conditions of the microwave changed between 180 and 900 W and 2–20 min [47,82]. The sonication time varied from 30 s to 30 min [41,43] and most sonication powers were lower than 140 W [40,41,83]. In this work, algal slurries were processed by microwave at 500 W and 600 W for 1 min. Also, ultrasonication was performed at 50, 75, and 134 W. The ultrasonic pretreatment time was 1 and 15 min. The microwave and ultrasonic processing were subjected to HTL at 350 °C for 35 min. The feedstock concentration and pressure were considered 8.6 wt% and 130 bar based on the optimum HTL condition which was reported for a brown macroalgae *Sargassum* [49].

Table 2
Biochemical component of Persian Gulf macroalgae species (as % of algal dry weight).

Algae	Biochemical component (wt%)				Reference
	Lipid	Protein	Ash	Carbohydrate[a]	
Caulerpa sertularioides	1.18	44.76	46.39	7.67	This study
Caulerpa racemosa	6.12	29.10	45.34	19.44	[57]
Caulerpa sertularioides	9.13	35.06	41.18	14.63	[57]
Galaxaura rugosa	4.02	17.82	38.31	39.85	[57]
Sargassum boveanum	2.02	21.33	49.14	27.51	[57]
Colpomenia sinuosa	3.45	11.57	26.31	58.67	[85]
Acanthophora spicifera	2.03	7.31	30.21	60.45	[85]
Champia parvula	4.26	16.52	39.65	39.57	[85]
Hypnea cervicornis	3.83	11.52	34.61	50.04	[85]
Gracillaria corticata	5.71	11.23	39.50	43.56	[85]
Jania rubens	1.52	10.12	44.13	44.23	[85]
Laurencia papillosa	3.70	12.23	32.20	51.87	[85]

[a] Calculated by the difference.

3. Results and discussion

3.1. Characteristics of algae

The biochemical components of algae include lipids, proteins, carbohydrates, moisture, and ash. *Caulerpa sertularioides* macroalgae used in this study constituted 1.02 % lipid, 38.5 % protein, 6.6 % carbohydrate, 13.98 % moisture, and 39.9 % ash by weight. The total lipid, protein, and ash contents (dry weight) of Persian Gulf macroalgae species are compared in Table 2. Results revealed that the native algal species has high protein (7.31 %–44.76 %), low lipid (1.18 %–9.13 %), and high ash (26.31 %–49.14 %) content. The biochemical result showed that the main biochemical components of *Caulerpa sertularioides* were ash and protein. Table 3 presents the result of C, H N, O elemental analysis of macroalgae. The macroalgae used in this research contained 25.93 % carbon, 3.58 % hydrogen, 2.52 % nitrogen, and 21.59 % oxygen by dry weight. It was found that the carbon element had a significant share, while nitrogen had a low content. The carbon content in the *Caulerpa sertularioides* was similar to *Ulva lactuca* [84] and *Solieria chordalis* [78]. The nitrogen content in *Caulerpa sertularioides* (2.52 %) was close to *Rhizoclonium riparium* (2.6 %), *Fucus ceranoides* (2.3 %), *Solieria chordalis* (2.7 %) [78], *Ulva lactuca and* (2.61 %) [84].

Also, the amount of hydrogen was very similar to the values presented for *Sargassum muticum* and *Solieria chordalisb* [78]. The high carbon and hydrogen contents in *Caulerpa sertularioides* highlight the attractive potential of this macroalgae to produce biocrude. Furthermore, the low nitrogen content improves the quality of produced biocrude which increases the calorific value and, as a result, reduces the emission of pollutants such as NOx [86]. Elemental analysis showed the high potential of *Caulerpa sertularioides* for biofuel production with relatively high yield and favorable quality.

The high HHV value represents the ability to produce biofuel with high amounts of energy. As shown in Table 3, the HHV of *Caulerpa sertularioides* was equal to 10.02 MJ/kg, higher than the HHV of *Fucus ceranoides*, *Sargassum muticum* (7.4 MJ/kg), and *Solieria chordalis* (7.3 MJ/kg) from Paignton [78]. The HHV of *Caulerpa sertularioides* was slightly less than *Enteromorpha prolifera* (12.15 MJ/kg) from the coast of the East Sea [15], *Rhizoclonium riparium* (12.20 MJ/kg) from Paignton [78]. The HHV of *Caulerpa sertularioides* indicates the suitability of Persian Gulf macroalgae for biofuel production.

Other characteristics of biomass that have a great effect on the extent of decomposition and destruction of biomass structure are the specific surface and porosity. Also, these properties can be used to compare the structure of the solid phase and the primary feedstock. The linear isotherm and the distribution trends of the pore volume and pore surface of algae are shown in Fig. S1 and Fig. S2 in the supplementary material. The specific surface area is equal to 2.269 m^2/g, which was close to the surface area of *Gelidium corneum* red macroalgae (2.19 m^2/g) [87] and *Sargassum* brown macroalgae (2.29 m^2/g) [49]. The adsorption average pore volume and pore width in this macroalgae were equal to 0.0043 cm^3/g and 35.2130 Å (3.52 nm).

3.2. Hydrothermal liquefaction results

Table 4 presents the data on product yields from HTL of *Caulerpa sertularioides* macroalgae, derived from systematically designed experimental conditions. Table 4 shows the yields of these experiments, providing a comprehensive overview of the HTL process efficiency under various operational parameters. As observed, the range of the biocrude yield varied between 4.88 and 22.12 wt%, the aqueous yield varied from 22.28 to 60.50 wt%, the solid yield changed from 37.79 to 19.81 wt%, and the gas yield ranged from 0.52 to 47.12 wt%.

The experimental conditions were subcritical experiments, while runs 6 and 13–16 in Table 4 were superheated steam hydrothermal processes and other experiments were subcooled water HTL under given pressure conditions. The superheated processes would directly affect the

Table 3
Elemental analysis and HHV of macroalgae species (as % of algal dry weight).

Macroalgae	C (wt%)	H (wt%)	N (wt%)	O (wt%)	Ash (wt%)	HHV[a] (MJ/kg)	References
Caulerpa sertularioides	25.93	3.58	2.52	21.58	46.39	10.02	This study
Enteromorpha prolifera	28.75	5.22	3.65	32.28	30.1	12.15	[15]
Oedogonium	39.6	5.8	1.1	45	9.1	15.79	[88]
Rhizoclonium riparium	26.8	5.1	2.6	21.0	44.5	12.20	[78]
Fucus ceranoides	28.4	3.9	2.3	52.8	12.6	8.7	[78]
Sargassum muticum	26.4	3.6	2.0	56.2	11.8	7.4	[78]
Solieria chordalis	25.3	3.5	2.7	51.4	17.1	7.3	[78]
Gracilaria gracilis	36.75	5.82	2.88	18.55	36	17.17	[79]
Cladophora glomerata	31.33	4.99	4.9	32.68	26.1	13.01	[79]
Ulva lactuca	25.31	5.44	2.61	–	–	–	[84]
Gracilaria corticata	26.46	5.01	1.89	–	–	–	[84]
Sargassum ilcifolium	26.20	4.52	1.88	–	–	–	[84]

[a] Calculated in this study.

Table 4
HTL experiment results of *Caulerpa sertularioides* macroalgae.

RUN	T (°C)	P (bar)	C_{Feed} (wt%)	Y_{BC} (wt%)	Y_{AP} (wt%)	Y_{SR} (wt%)	Y_G (wt%)	$\frac{Biocrude}{Solid}$	Phase
1	215.91	100	6.5	5.09	52.26	37.79	4.86	0.13	Subcooled
2	250	50	3	5.21	51.62	32.46	10.71	0.16	Subcooled
3	250	50	10	5.38	60.50	33.60	0.52	0.16	Subcooled
4	250	150	10	6.37	59.79	32.35	1.49	0.20	Subcooled
5	250	150	3	6.22	56.03	30.35	7.4	0.20	Subcooled
6	300	15.91	6.5	7.02	38.33	29.17	25.48	0.24	Superheated
7	300	100	0.61	4.88	50.19	20.86	24.07	0.23	Subcooled
8	300	100	6.5	7.89	40.58	22.13	29.4	0.36	Subcooled
9	300	184.09	6.5	14.10	46.05	20.92	18.93	0.67	Subcooled
10	300	100	6.5	7.08	42.20	22.07	28.65	0.32	Subcooled
11	300	100	6.5	7.88	42.99	21.41	27.72	0.37	Subcooled
12	300	100	12.38	6.89	43.05	25.77	24.29	0.27	Subcooled
13	350	150	10	22.12	25.56	19.81	32.51	1.12	Superheated
14	350	50	3	6.66	28.56	20.94	43.84	0.32	Superheated
15	350	150	3	10.02	26.23	19.99	43.76	0.50	Superheated
16	350	50	10	9.68	22.28	20.92	47.12	0.46	Superheated
17	384.09	100	6.5	14.28	30.13	20.40	35.19	0.70	Superheated

biocrude-solid ratio. The result shows the biocrude-solid ratio changed from 0.13 to 1.12 with higher values for experiments in superheated conditions. In subcooled conditions, the ratio of biocrude to solids ranged from 0.16 to 0.2 when pressure changed between 50 and 150 bar at 250 °C, irrespective of variations feed concentration. It varied between 0.23 and 0.37 at 300 °C, having a higher value for higher pressures and feed concentrations. The findings align with those reported by Ocfemia et al. [89], which demonstrated that enhanced pressure improved oil yield at subcooled conditions with operating temperatures of 285 °C and 305 °C. The highest biocrude-to-solid ratio of 0.67 was obtained at 300 °C and 184 bar. The results showed that high pressure leads to effective decomposition and extraction of biomass at higher temperature in subcooled conditions. Thus, more biocrude and less solid were produced, resulting in the highest biocrude-to-solid ratio under subcooled conditions. Despite observing a comparable trend under superheated conditions, the ratio was higher than that observed under subcooled conditions. When the feed concentration ranged from 3 to 10 wt%, elevating the pressure to 150 bar led to an enhanced biocrude-to-solid ratio to 1.12 at a temperature of 350 °C. In superheated conditions, the solid yields fluctuated around 20 wt%. Although the solid yields did not change much, the share of liquid and gas products changed significantly. The highest biocrude yield was obtained at 350 °C and 150 bar, resulting in the maximum biocrude-to-solid ratio under superheated conditions.

3.2.1. Biocrude prediction model

The experimental data was subjected to analytical scrutiny using version 13 of the Design-Expert software, which employed a multifaceted regression analysis technique. Additionally, within this computational platform, evaluations to determine the statistical significance of the regression model were performed. Results showed that the inverse model was a better choice for predicting the results of the HTL biocrude yield with the highest regression (0.9939). Furthermore, R^2, adjusted-R^2, predicted-R^2, and predicted residual error sum of square (PRESS) for the inverse model are presented in Table S3 in the supplementary material. The quadratic equation presented better prediction accuracy based on adjusted-R^2, and predicted-R^2. The adjusted-R^2 and predicted-R^2 are equal to 0.986 and 0.974 for the quadratic inverse model. As shown in Table S3, the lowest value of PRESS of 0.0009 for the quadratic model showed that this statistical model was a better fit for the data.

The normal plot, residuals vs. the run, and residuals vs. predicted are presented in Figs. S3–S5 in the supplementary material. These figures confirmed the adequacy of the inverse quadratic model because of the random distribution of results in these graphs. All data were scattered without a specific pattern within the acceptable limits of the process. Fig. S6 shows model predictions vs. actual values. The closeness and agreement of obtained values with the predicted line indicate the correctness of the selected model. Therefore, the selected model was well-matched with the experiment results.

The variance of the model is presented in Table S4. The selected model was significant, while the lack of fit was not significant. This result confirmed the adequacy of the selected model. Also, according to low P-values (<0.0001), reaction temperature, pressure, and feed concentration were effective parameters. The terms with P-value >0.05 such as A^2 and BC were not significant in the biocrude model. After ignoring these parameters, coefficients were adjusted. Table 5 shows the ANOVA of the biocrude yield model. An empirical correlation was

Table 5
Adjusted ANOVA results for biocrude yield.

	Sum of squares	df	Mean square	F-value	P-value	
Model	0.0345	7	0.0049	207.02	<0.0001	significant
A-Temperature (°C)	0.0190	1	0.0190	797.15	<0.0001	
B-Pressure (bar)	0.0061	1	0.0061	256.34	<0.0001	
C-Feed concentration (wt%)	0.0033	1	0.0033	137.95	<0.0001	
AB	0.0003	1	0.0003	12.34	0.0066	
AC	0.0010	1	0.0010	43.76	<0.0001	
B^2	0.0011	1	0.0011	44.45	<0.0001	
C^2	0.0027	1	0.0027	114.20	<0.0001	
Residual	0.0002	9	0.0000			
Lack of Fit	0.0001	7	0.0000	0.1596	0.9725	not significant
Pure Error	0.0001	2	0.0001			
Cor Total	0.0347	16				

obtained to predict the biocrude yield based on the quadratic model (Eq. (11)).

$$\frac{1}{Y_{BC}} = 0.2408 - 0.00007\,A + 0.0010\,B - 0.0006\,C - 2.4240\times10^{-6}AB - 6.5210\times10^{-6}\,AC - 3.7024\times10^{-6}B^2 + 0.0012\,C^2 \quad (11)$$

where Y_{BC} is biocrude yield (wt%), A, B, and C are temperature (°C), pressure (bar), and feed concentration (wt%). The interaction term was denoted as AC.

3.2.2. HTL byproduct prediction models

The aqueous phase, solid residue, and gas phase yield models are presented in this section. The linear model was more accurate for the yield of the aqueous phase and gas phase, while the quadratic model could predict solid residue yield well. ANOVA and statistical analysis for biocrude, solid residue, aqueous-phase, and gas-phase yield models are presented in Tables S4–S7 in the supplementary material. The P-value was less than 0.0500, which indicates the models were significant. Moreover, the quadratic ($R^2 = 0.97$), linear ($R^2 = 0.82$), and linear ($R^2 = 0.83$) equations were recognized as the best models for solid residue, aqueous phase, and gas yield prediction, respectively. The adjusted-R^2 was in agreement with the predicted-R^2 for HTL product yields. The adjusted-R^2 and predicted-R^2 differences were less than 0.2. Adequate

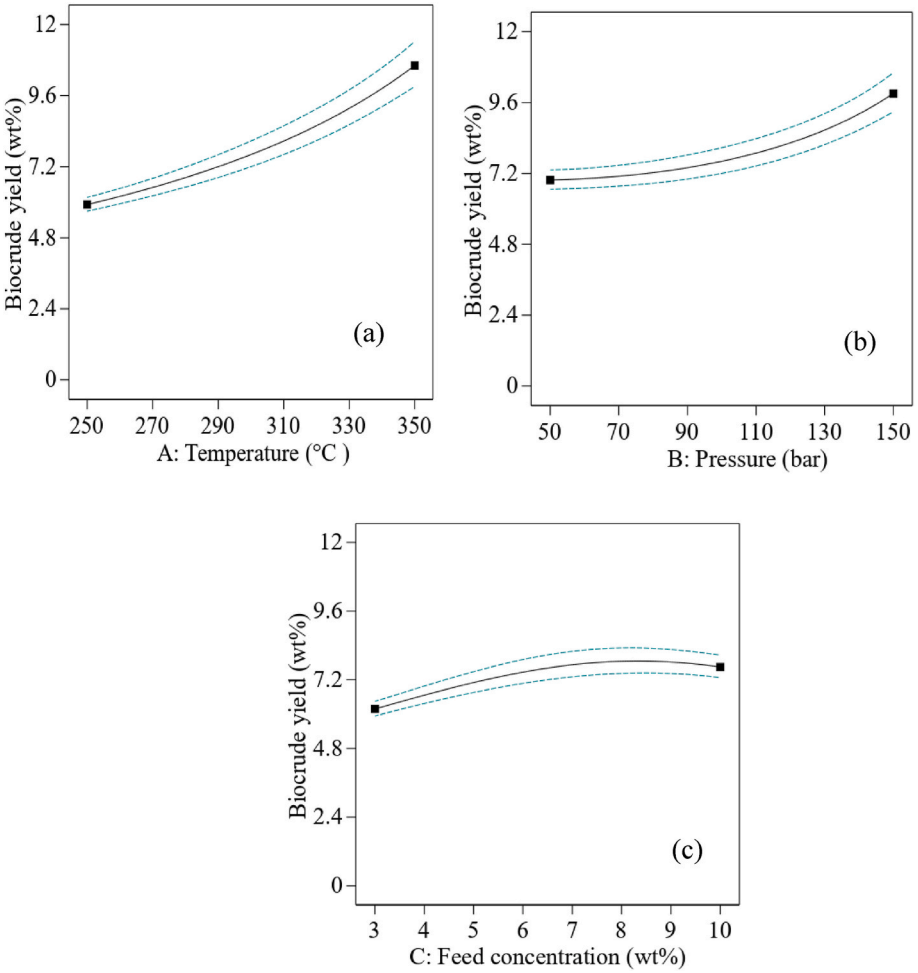

Fig. 2. Change in biocrude yield by a) temperature at 100 bar and 6.5 wt% b) pressure at 300 °C and 6.5 wt%, and c) feed concentration at 300 °C and 100 bar.

precision measures signal-to-noise ratio and desired adequate precision is greater than 4. The adequate precision of solid residue, aqueous phase, and gas phase indicated an adequate signal. These models can be used to navigate the design space. The results showed that among the operating parameters, temperature with a P-value <0.0001 had the greatest effect on the solid, aqueous phase, and gas yield. The pressure effect was more influential on solid yield. However, feed concentration had a negligible effect on HTL byproduct yields. The results of ANOVA for adjusted models were presented in Tables S8–S10 in the supplementary material. The normal plot, residuals vs. the run, and residuals vs. predicted figures of solid residue, aqueous phase, and gas phase yield are given in Figs. S7–S15 in the supplementary material. The aqueous phase, solid residue, and gas phase yields were calculated by Eq. (12)–(14).

$$Y_{SR} = 149.3418 - 0.6976\,A - 0.1090\,B + 0.2340\,C + 0.0009\,A^2 + 0.0004\,B^2 \quad (12)$$

$$Y_{AP} = 113.5468 - 0.2380\,A \quad (13)$$

$$Y_G = -61.1116 + 0.2821\,A \quad (14)$$

where Y_{SR}, Y_{AP}, and Y_G are solid residue, aqueous phase, and gas phase yields.

3.2.3. Effect of parameters on HTL

In this section, the influence of operating factors and the binary interactions of these parameters on the product yield obtained from HTL of *Caulerpa sertularioides* macroalgae has been investigated. The effect of operating parameters on biocrude and other HTL products is shown in Fig. 2 and Figs. S16–S18 in supplementary material, respectively.

3.2.3.1. Temperature. Thermal conditions stand as the paramount factor influencing HTL and induce significant changes in product yield in subcooled and superheated conditions. The temperature effect on biocrude yield at 100 bar is presented in Fig. 2a. As can be seen, in superheated conditions (the temperature range from 315 °C to 350 °C), the biocrude yield increased at a steeper rate than subcooled. This is because higher temperatures typically accelerate chemical reaction rates. The breakdown of organic substances into smaller molecular structures, followed by their reassembly into biocrude above 300 °C, might proceed with greater efficiency, potentially resulting in a higher yield [1]. High temperatures (above 300 °C) are likely high enough to initiate and sustain endothermic reactions that are essential for breaking down complex organic structures into simpler hydrocarbons, leading to increased biocrude production [21]. The overall results showed that elevated temperatures were conducive to the enhancement of biocrude and gaseous yields. Conversely, there was a discernible reduction in the yield of both the aqueous and solid phases. This implies that at constant pressure and biomass concentration, a thermal elevation from 250 °C to 350 °C significantly enhances the production of biocrude and gaseous yields, with gas yields showing a dramatic increase. Superheated water has a lower dielectric constant, which reduces the solvation of ions and polar molecules, leading to a higher concentration of free radicals, which may favorable for gasification [90]. A similar trend was observed by Nazari et al. [91]. Investigations revealed an enhanced efficacy in the hydrolytic breakdown of biomass when subjected to elevated thermal conditions. This absorption of heat facilitates the disintegration of the biomass's structural integrity, subsequently promoting the transposition of its constituents into both biocrude and gaseous states [91]. Additionally, empirical evidence suggests that a rise in temperature acts as a catalyst for the transformation of low-molecular-weight substances into more complex molecular entities through a series of repolymerization processes. This observation is consistent with findings in the literature [62,92–94].

3.2.3.2. Pressure. Reactor pressure significantly influences the HTL of biomass. Experiments were performed at a pressure range of 50–150 bar to explore the influence of pressure. In this study, operational constraints were imposed on the reactor to prevent the internal pressure from exceeding 200 bar. This precautionary measure was in adherence to the upper-pressure limits recommended by the equipment's manufacturer for safe operation. Fig. 2b presents the effect of pressure on biocrude yield at 300 °C. The biocrude and aqueous phase yields were slightly enhanced by increasing pressure, while high pressure was detrimental to gas and solid production under subcooled conditions. Under conditions of superheating (with pressures varying between 90 bar and 150 bar), the production of biocrude exhibited a more pronounced increase compared to that under subcooled conditions. There are few studies were conducted under superheated process. For instance, Qian et al. [31] investigated the effects of reactor pressure on HTL of sewage sludge and stated that biocrude yield increased significantly when pressure went up from 200 to 220 bar under superheated conditions. In the study conducted by Qian et al. [31], a comparable pattern was observed for superheated conditions. Also, water density in the HTL reactor increases with increasing pressure, and higher water density favors the decomposition and extraction of biomass [95]. The biomass converted into biocrude and aqueous phase easily at high pressure, because more force was applied to destroy the bonds of biomass [8]. As a result, the tendency to gasification decreased as the pressure increased. However, the influence of pressure on gas yield was small. This outcome is in agreement with the literature [31,96].

3.2.3.3. Feedstock concentration. Among the three parameters investigated in HTL, feed concentration had the least influence on the yield of HTL products. Fig. 2c shows that a slight change was observed in the HTL biocrude. However, a higher feed concentration led to higher biocrude and solid residue yields. Valdez et al. [97] indicated an increase in biocrude yields by increasing the biomass-to-solvent ratio. Although changes in feed concentration did not affect the aqueous phase, the gas yield reduced with increasing biomass concentration. A similar trend was obtained by Qu et al. during the HTL of woody biomass [98]. Results showed that the maximum biocrude was obtained at 7.5 wt% of *Caulerpa sertularioides* macroalgae concentration at 300 °C and 100 bar. This observation is confirmed by Mastalinezhad et al. [49] who mentioned that the maximum biocrude yield was obtained at 300 °C when using 7.5 wt% of feedstock concentration.

3.2.3.4. Parameter interactions. Each process parameter was analyzed individually while keeping the others fixed. In this section, the interaction of parameters on the HTL performance in terms of product yield is examined. The contour plots of interaction between parameters are presented in Figs. S19–S21 in the supplementary material.

3.2.3.4.1. Temperature and pressure interaction. The interaction of temperature and pressure on biocrude and other HTL products is presented in Fig. 3 and Fig. S22, respectively. All interaction effects are

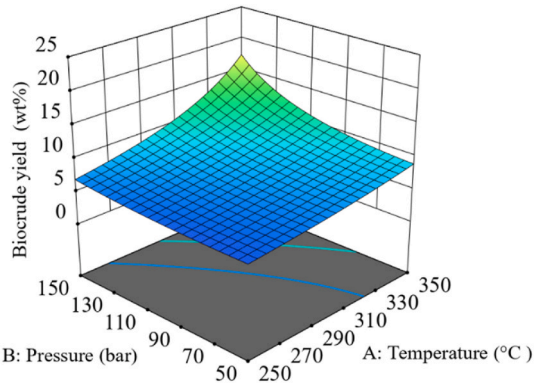

Fig. 3. Temperature and pressure interaction effect on biocrude.

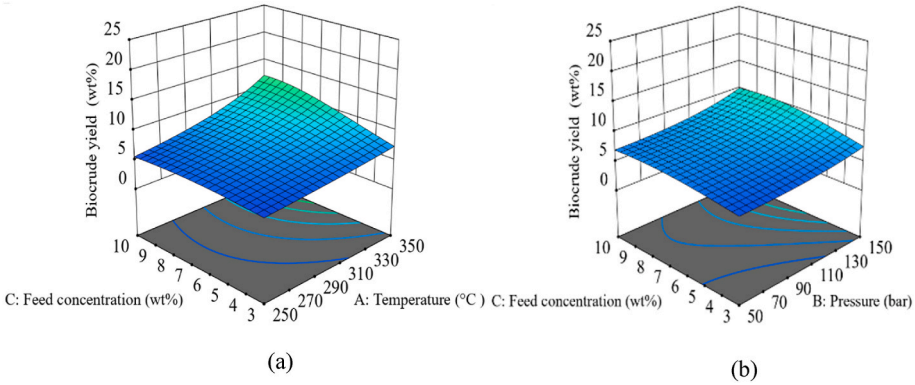

Fig. 4. The effect of a) the temperature and feed concentration interaction and b) the pressure and feed concentration interaction on biocrude yield.

shown in the central point of feed composition (6.5 wt%). Results show that biomass decomposes more to HTL products by increasing temperature and pressure. The maximum biocrude of 17.35 wt% was obtained at 350 °C and 150 bar. However, HTL favored the aqueous phase production at low temperatures and high pressure. The HTL process with 6.5 wt% of biomass concentration produced the maximum aqueous phase yield (55.31 wt%) at 250 °C and 150 bar. At minimal temperatures and pressures, the destruction of biomass is significantly impeded. As a result, solid residue yield was a maximum of 32.25 wt% at 250 °C and 50 bar. Moreover, the gas yield decreased at low temperatures and high pressure. The minimum gas yield (7.13 wt%) was predicted at 250 °C and 150 bar.

3.2.3.4.2. Temperature and feed concentration interaction. The interaction of feed concentration with pressure and temperature for biocrude and solid residue are shown in Fig. 4 and Fig. S23, respectively. Fig. 4a presents the temperature and feed concentration interaction on biocrude. All interaction effects were studied in the central point of pressure (100 bar). The minimum solid residue yield was obtained at high temperatures and high feed concentrations. Also, the highest biocrude yield of 10.30 wt% was predicted at 350 °C and 10 wt% biomass concentration. A similar result was reported by Jena et al. [99] and Anastasakis and Ross [100], where the maximum biocrude yield was obtained at 350 °C and 10 wt% feed concentration. Also, a close result was obtained by Qu et al. [98] during the HTL of woody biomass, where the maximum biocrude yield at 340 °C was obtained with 9 wt% of biomass concentration. Anastasakis and Ross [100] indicated that the highest biocrude yield was accomplished by adding 9.1 wt% of reactor loading at 350 °C.

3.2.3.4.3. Pressure and feed concentration interaction. The interaction of pressure and feed concentration for biocrude are indicated in Fig. 4b. Results reveal that this interaction had a low effect on biocrude and solid residue yields.

Just one study was found to consider an interaction of pressure and feed concentration simultaneously. Chan et al. [93] studied the production of bio-oil from palm kernel shells via HTL. Their findings indicated that at a lower biomass-to-water ratio of 0.20, elevating the pressure from 25 to 35 MPa had a minimal impact on the yield of bio-oil at 360 °C. Conversely, at a higher biomass-to-water ratio of 0.50, the reduction in bio-oil yield became more pronounced with an increase in pressure because of a diminished liquefaction efficiency at this particular biomass-to-water ratio [93]. In comparison with the results of Chan et al. [93], the maximum biocrude was predicted at high pressure and feed concentration at the central point of 300 °C in this study. These contradictory results may refer to different operation ranges performed in the HTL experiments. The highest solid yield of 25 wt% was obtained at lower pressure and higher feed concentration. This is because the cellular membrane disruption of feed components is not provided at lower pressure, and they remain in as solid phase, which results in a lower biocrude yield.

Table 6
Comparing the experiment and RSM predicted product yields.

Condition	T (°C)	P (bar)	C_{Feed} (wt%)	Y_{BC} (wt%)	Y_{AP} (wt%)	Y_{SR} (wt%)	Y_G (wt%)
Predicted HTL yield	350	150	9.752	22.41	31.10	19.74	26.75
Experiment HTL yield	350	150	9.752	22.15	26.46	19.79	31.60
Error %				1.17	17.53	0.25	15.34

3.2.4. HTL optimization

Two optimization for subcooled and superheated conditions were performed, before overall optimization being done. The optimization results for subcooled conditions showed that the highest biocrude of 10.62 wt% was predicted at 300, 150 bar, and 8.86 wt% of feed concentration, while that for superheated conditions was obtained at 24.60 wt% at 350 °C, 150 bar, and 10 wt% of feed concentration. The optimum biocrude-to-solid ratio was predicted at 0.47 under subcooled conditions, while that was reported at 1.29 under superheated conditions. The overall optimization results indicate that the optimum conditions for maximum biocrude yield were 350 °C, 150 bar, and 9.752 wt% of feed concentration. The close result of optimum conditions was reported by Bach et al. [101], Jazrawi et al. [10], and Biller and Ross [102]. Moreover, Wei and Jie showed that in optimum conditions of 10.5 % concentration, 357 °C, and 37 min, the highest biocrude yield was obtained using the fresh microalgae [92].

Table 6 compares the predicted model and experiment results. Under optimum conditions, RSM predicted 22.41, 31.10, and 19.74 wt% for biocrude, aqueous phase, and solid residue, respectively. The predictive gas yield was calculated at 26.75 wt% by differences. However, the experiment result indicated that the biocrude, aqueous phase, solid residue, and gas yield were 22.15, 26.46, 19.79, and 31.60 wt% under optimum conditions. The biocrude yield of *Caulerpa sertularioides* was close to the HTL biocrude yield of *Enteromorpha prolifera* (23.0 wt%) at 300 °C [15] and slightly lower than the biocrude yield of *Cladophora vagabunda* (26.2 wt%) at 340 °C and 140–170 bar [103]. The percentage of error shows that solid and biocrude yield models have high accuracy. The difference between predicted and experiment yields for gas and aqueous phase were obtained at just above 4.6 wt%. The over-prediction of the model for the aqueous phase was previously seen at reaction times of about 30 min [21]. The low accuracy for the gas phase may refer to the difficulty of gas measuring, which is usually calculated by difference. Results showed that the maximum yield of biocrude produced in this study was higher than the values of HTL for *Fucus serratus* (16.5 wt%) [104], *Eucheuma denticulatum* (18.5 wt%) [105], *Sargassum tenerrimum* (16.33 wt%) [106], *Ulva prolifera* (12.0 wt%) [107], *Laminaria saccharina* (19.3 wt%) [100], *Laminaria japonica* (15.32 wt%) [108], *Derbesia tenuissima* (19.7 wt%), *Ulva ohnoi* (18.7 wt%), *Chaetomorpha linum* (9.7

Table 7
Elemental composition, HHV, and ER of biocrude.

RUN	T (°C)	P (bar)	C_{Feed} (wt%)	C (wt%)	H (wt%)	N (wt%)	O (wt%)	H/C	N/C	O/C	HHV (MJ/kg)	ER%
1	215.91	100	6.5	63.22	8.08	3.7	25	0.13	0.06	0.40	28.95	14.71
2	250	50	3	64.49	8.46	3.34	23.71	0.13	0.05	0.37	29.98	15.59
3	250	50	10	64.19	8.21	3.95	23.65	0.13	0.06	0.37	29.58	15.88
4	250	150	10	64.44	7.65	4.13	23.78	0.12	0.06	0.37	28.99	18.43
5	250	150	3	64.54	10.29	2.15	23.02	0.16	0.03	0.36	32.24	20.02
6	300	15.91	6.5	69.97	8.81	2.65	18.57	0.13	0.04	0.27	32.85	23.01
7	300	100	0.61	71.67	8.85	3.35	16.13	0.12	0.05	0.23	33.73	16.43
8	300	100	6.5	66.74	7.72	4.07	21.47	0.12	0.06	0.32	30.11	23.71
9	300	184.09	6.5	77.02	11.26	2.54	9.18	0.15	0.03	0.12	39.17	55.12
10	300	100	6.5	65.1	7.36	3.99	23.55	0.11	0.06	0.36	28.90	20.42
11	300	100	6.5	66.91	7.44	4.19	21.46	0.11	0.06	0.32	29.84	23.47
12	300	100	12.38	63.15	7.57	4.25	25.03	0.12	0.07	0.40	28.31	19.47
13	350	150	10	72.87	7.91	4.35	14.87	0.11	0.06	0.20	30.59	73.19
14	350	50	3	74.71	7.73	3.84	13.72	0.10	0.05	0.18	33.16	22.41
15	350	150	3	68.63	7.81	3.7	19.86	0.11	0.05	0.29	31.05	31.05
16	350	50	10	70.05	8.83	3.51	17.61	0.13	0.05	0.25	32.98	31.87
17	384.09	100	6.5	73.43	8.5	4.45	13.62	0.12	0.06	0.19	34.17	48.70

wt%), *Cladophora coelothrix* (13.5 wt%), and *Oedogonium* sp. (19.7 wt%) [103] macroalgae. Therefore, *Caulerpa sertularioides* macroalgae gives good performance for a future biorefinery.

3.3. Biocrude characterization

In this section, the characteristics of biocrude are discussed. Elemental analysis was performed for all runs to calculate HHV and ER. However, FT-IR, GC-MS, and TGA results of biocrude were reported at optimized operating conditions.

3.3.1. Elemental analysis, HHV, and ER calculation

Determining the concentration of biocrude elements leads to a better understanding of the characteristics of biocrude. In addition, it is possible to examine the mechanisms of biocrude production and the amount of heating value. Table 7 lists elemental composition, HHV, and ER for biocrude obtained from HTL at different experimental conditions. It should be noted that the sulfur content of the biocrude was below the detection limit.

As shown in Table 7, biocrude had a range of 63–74 %, 7–11 %, 2–4.5 %, and 9–25 % for carbon, hydrogen, nitrogen, and oxygen, respectively. Elemental analysis showed that compared to the initial feed, the amount of carbon and hydrogen elements in the biocrude increased sharply while the amount of oxygen decreased compared to the oxygen of algae. Oxygen was consistently eliminated through the processes of dehydration and decarboxylation [109]. The nitrogen contents slightly increased compared to dry algae, indicating that the removal of N was not as effective as deoxidation during HTL. The elemental analysis showed that carbon contents had a significant share of the constituent elements of biocrude and increased with temperature. The carbon content increased from 63.22 wt% to 73.43 wt% when temperature varied between 250 °C and 384 °C. Similar results previously were reported by Yang et al. [109], Anastasakis and Ross [110], and Zhu et al. [111]. Also, higher temperatures facilitated deoxygenation as oxygen content reduced from 25 % at 215 °C to 13.62 % at 384 °C.

The H/C atomic ratio fluctuates in the range of 1.10–1.15, which is below the average of H/C (1.65) in petroleum [112]. For comparison, the H/C ratio of petroleum crudes ranges from 1.4 to 1.9 [113]. A primary factor contributing to the inadequate increase in hydrogen concentration, which remained at approximately 8 % within the biocrude, was its insensitivity to fluctuations in temperature and pressure. Introducing a catalyst along with supplemental hydrogen during the HTL process may enhance the hydrogenation of the biocrude [114]. The N/C atomic ratio varied from 0.03 to 0.07, which was higher than the range of 0.001–0.02 N/C in petroleum [112,113]. The high N/C ratio mainly results from the high nitrogen content (2.52 %) in the algal feedstock. The O/C ratio changed from 0.12 to 0.4. More severe HTL conditions drove more of the oxygen atoms out of the biocrude, but the O/C ratio still exceeded the 0.0004–0.01 O/C ratio for petroleum crude oils [113]. However, biocrude had a high oxygen and nitrogen content. Thus, upgrading is needed to create oils with lower O/C and N/C ratios to are comparable to those in petroleum-derived oils [113].

The quality and energy recovery of biocrude is important. As shown in Table 7, HHVs ranged from 28.31 to 39.17 MJ/kg, which is higher than the HHVs biocrude from *Sargassum tenerrimum* (22–27 MJ/kg) [115], and *Enteromorpha prolifera* (22–27 MJ/kg) [109]. Also, HHVs of biocrude were much higher than feedstock (10.02 MJ/kg). The highest HHV (39.17 MJ/kg) was obtained at 300 °C, and 184 bar, while HHV slightly decreased to 34.17 MJ/kg at 384 °C, 100 bar, and 6.5 wt% of feed concentration, and 33.16 MJ/kg at 350 °C, 150 bar, and 10 wt% of algal feed concentration. These results are consistent with the conversion of lipid-bound fatty acids to free acids at temperatures above 300 °C [116], and dehydration, rearrangement, decomposition, and conversion of saturated bonds into unsaturated bonds, resulting in lower HHVs for oils from higher temperatures, most notable at 350 °C [117]. The HHV (33.16 MJ/kg) of *Caulerpa sertularioides*-derived biocrude at 350 °C, 150 bar and 10 wt% feed concentration was close to the HHV of biocrude obtained from marine green macroalgae *Derbesia* (33.2 MJ/kg), *Ulva* (33.8 MJ/kg), *Chaetomorpha* (32.5 MJ/kg), *Cladophora* (33.3 MJ/kg) at 350 °C, 250 bar and 6.67 wt% [103]. Furthermore, ERs use the amount of produced biocrude and take its heating value into account. The values for the ER of *Caulerpa sertularioides* ranged from a low value of 14.71 % at 215 °C, to 73.19 % at 350 °C. Although, temperature and pressure had a strong effect on HHV, an increase in algae content did not appear to impact energy recovery. The higher energy of 31–73 % was recovered at the higher temperatures than that of 14–20 % at the lower temperatures. The maximum HHV of 73.19 % was obtained at high temperatures and pressure (350 °C and 150 bar), which was higher than those in previous studies [118–121]. The ER represents that *Caulerpa sertularioides* has considerable potential to produce biocrude with great quantity and quality.

3.3.2. FT-IR analysis

The FT-IR spectra of biocrude feed reveals distinct absorption bands indicative of specific functional groups, signifying the existence of particular classes of compounds within the sample. The FT-IR spectra of the biocrude are shown in Fig. 5. The absorbance peaks at around 3200 cm^{-1} were observed in biocrude spectra, corresponding to O-H or N-H stretching vibrations in carboxyl, hydroxyl, and amino groups [27], which were abundant in molecules of acids, and N-containing heterocyclic compounds that were detected by GC–MS. The N-H bending

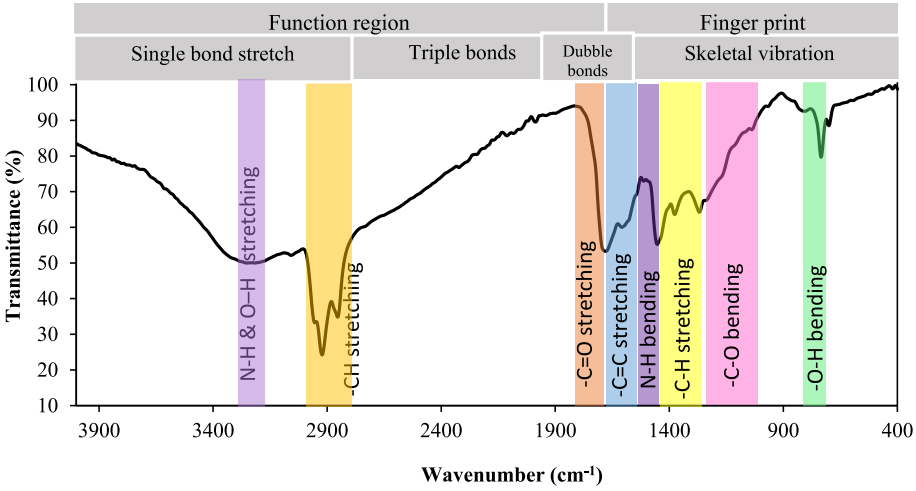

Fig. 5. FT-IR spectra of biocrude.

vibration peak at 1511–1679 cm^{-1} indicated the presence of N-containing compounds [75,122]. The weak absorbance peak at 3216 cm^{-1} is attributed to the O–H vibration caused by water and alcohol in the biocrude. Also, the strong absorbance peak of C–H stretching vibrations between 2854 and 3058 cm^{-1} represent the CH_3 and CH_2 groups [15]. The intense absorbance C=O vibration at 1818 cm^{-1} in biocrude suggests that a lot of ketones and aldehydes are produced by the decomposition of proteins in raw materials [76]. The C=C stretching vibrations at 1511, 1608, and 1679 cm^{-1} in biocrude indicate alkenes. Moreover, the presence of C–H bending vibrations between 1376 and 1452 cm^{-1} indicates the presence of alkanes. The bands at 1039 and 1268 cm^{-1} may be attributed to C–O vibrations, suggesting the presence of functional groups typically found in esters, acids, or alcohols within the biocrude composition [81]. Also, the bands at around 700 and 806 cm^{-1} in the biocrude due to O–H bending indicate the presence of phenols, ethers, esters, and aromatic compounds. Similar results are seen for different macroalgae. For instance, the FT-IR result reported for biocrude from green macroalgae *Chaetomorpha* sp. [123] showed that the significant peaks observed at 2926 cm^{-1} and 2858 cm^{-1} corresponded to the C–H, a strong absorbance peak at 1674 cm^{-1} that attributed to C=O, the C–H bending at 1460 cm^{-1} and 1388 cm^{-1} with the C–O bending at 1000–1300 cm^{-1} suggested the presence of acids and ester group, and the aromatic C=C stretching observed at 1521 cm^{-1}. The FT-IR result of biocrude from brown macroalgae *Sargassum* sp. indicated that its peaks at 722, 737, and 819 cm^{-1}, O–H bending, showed the presence of aromatic compounds, phenols, esters, and ethers; at 1265 cm^{-1}, C–O stretching for alcohols and with peaks at 1383 and 1458 cm^{-1}, C–H bending; alkenes were detected at 1625 cm^{-1}, C=C stretching; ketones, aldehydes, and carboxylic acids with peak at 1688 cm^{-1}, C=O stretching; alkanes were found at 2875, 2932, and 2965 cm^{-1}, C–H stretching and water with the peak at 3375 cm^{-1} [124].

3.3.3. GC-MS analysis

GC-MS analysis was carried out to confirm the finding from FT-IR by gaining further insight into the identification of biocrude compounds obtained from HTL of *Caulerpa sertularioides* at 350 °C and 150 bar. Components were characterized by comparing their principal peaks with reference spectra in the NIST mass spectral database. The biocrude contained ketones, esters, acids, aldehydes, alcohols, hydrocarbon, and nitrogen-containing compounds. The major components of biocrude are shown in Table 8. It was clear that most constituents of the biocrude were complex cyclic compounds. The main functional groups include acids, n-containing heterocyclic compounds, and ketones, which were similar to that of the biocrude obtained from *Enteromorpha prolifera* [109], *Sargassum tenerrimum* [125], and *Ulva prolifera* [107] macroalgae.

Table 8
Compounds identified from the biocrude obtained from HTL of Caulerpa sertularioides at optimum condition by the GC-MS analysis.

Classification	Compound name	Chemical formulas	Area (%)
Ketones	2-Cyclopenten-1-one, 3-methyl-	C_6H_8O	1.02
	2-Cyclopenten-1-one, 2,3-dimethyl-	$C_7H_{10}O$	5.91
	2-Cyclopenten-1-one, 2,3,4-trimethyl-	$C_8H_{12}O$	0.68
	2-(2-Methyl-propenyl)-cyclohexanone	$C_{10}H_{16}O$	0.56
	Spiro[5.5]undecane-1,7-dione	$C_{11}H_{16}O_2$	0.58
	1H-Inden-1-one, 2,3-dihydro-3-methyl-	$C_{10}H_{10}O$	1.36
Aldehydes	2,4-Heptadienal, (E,E)-	$C_7H_{10}O$	1.00
Esters	2(3H)-Benzofuranone, hexahydro-3-methylene-	$C_9H_{12}O_2$	1.85
	7-Methyl-Z-tetradecen-1-ol acetate	$C_{17}H_{32}O_2$	0.88
Amines	3-Buten-2-amine, 4-(2,6,6-trimethyl-1-cyclohexen-1-yl)-	$C_{13}H_{23}N$	0.32
Acids	Tetradecanoic acid	$C_{14}H_{28}O_2$	3.58
	9-Hexadecenoic acid	$C_{16}H_{30}O_2$	4.10
	n-Hexadecanoic acid	$C_{16}H_{32}O_2$	48.75
Alcohols	1-Hexadecanol, 2-methyl-	$C_{17}H_{36}O$	5.30
	1-Dodecanol, 3,7,11-trimethyl-	$C_{15}H_{32}O$	4.71
Others	Cyclopropa[d]naphthalen-3-one, octahydro-2,4a,8,8-tetramethyl-, oxime	$C_{15}H_{25}NO$	0.66
	1H-Indole, 5,7-dimethyl-	$C_{10}H_{11}N$	2.03
	2,3,7-Trimethylindole	$C_{11}H_{13}N$	1.02
	1H-Indole, 5,6,7-trimethyl-	$C_{11}H_{13}N$	1.88
	Quinoline, 1,2-dihydro-2,2,4-trimethyl-	$C_{12}H_{15}N$	0.90
	1-Benzoylamino-5-piperidinyl-1-phenylpentane	$C_{23}H_{30}N_2O$	0.54
	9-Oxabicyclo[3.3.1]non-6-en-2-one, oxime	$C_8H_{11}NO_2$	6.76
	Phorbol	$C_{20}H_{28}O_6$	0.48
	1-Propanone, 1-(2-methylphenyl)-2-methyl-3-(1-piperidyl)-	$C_{16}H_{23}NO$	2.46
	Piperacetazine	$C_{24}H_{30}N_2O_2S$	1.73
	Ergost-14-ene, (5.alpha.)-	$C_{28}H_{48}$	0.94

The main components were n-Hexadecanoic acid (48.75 %), 9-Oxabicyclo [3.3.1] non-6-en-2-one oxime (6.76 %), 2-Cyclopenten-1-one 2, 3-dimethyl- (5.91 %), 1-Dodecanol, 3,7,11-trimethyl- (4.54 %), 1-Hexadecanol 2-methyl- (4.71 %), 9-Hexadecenoic acid (4.10 %) and Tetradecanoic acid (3.58 %). Hexadecanoic acid, a predominant constituent frequently identified in bio-oil derived from algal sources, stands out as a significant molecular entity [107,126,127].

The mechanism of the various reactions occurring during HTL of algae is difficult to describe because the reaction pathways are multifold [50]. The HTL involves a complex array of sequential and parallel reactions that are influenced by the feedstock's composition and operating conditions. The high temperatures and pressures utilized in the HTL process alter the structure of long-chain polymers composed of hydrogen, oxygen, and carbon into short-chain hydrocarbons [128]. The major HTL reaction pathways are depolymerisation (hydrolysis), decomposition, and recombination (repolymerization) [129]. Through depolymerisation, long-chain polymers are broken down into oligomers that can dissolve in water. This transformation allows carbohydrates to be broken down into monosaccharides and polysaccharides; proteins are reduced to peptides and amino acids; and lipids are separated into fatty acids and glycerol [130]. The hydrolyzed monomers undergo further breakdown through the elimination of water (dehydration), carbon dioxide (decarboxylation), and the removal of amino groups (deamination) by decomposition [131]. These processes of dehydration and decarboxylation contribute to a reduction in oxygen levels. Various reactive fragments formed through decomposition processes start to recombine (undergo repolymerization) at temperatures exceeding 300 °C, leading to the synthesis of biocrude constituents [1]. In this study, GC-MS analysis indicated three likely pathways for the identified compounds. In the first pathway, fatty acids, like hexadecanoic acid and tetradecanoic acid, are generally produced from the hydrolysis of lipids in the raw material [109]. Subsequently, these compounds undergo reactions with carbohydrates, potentially forming additional compounds such as 7-methyl-Z-tetradecen-1-ol acetate and 2(3H)-benzofuranone, hexahydro-3-methylene. In the second pathway, nitrogenated compounds are formed by decarboxylation, deamination, dehydration, depolymerisation, and decomposition reactions of proteins [9]. After temperature increases in the HTL reactor, protein dehydrates to amino acids and then based on the Maillard reaction goes on to react with the carbohydrates [132]. The Maillard reaction is capable of generating various types of nitrogen-containing heterocyclic compounds, like piperacetazine and quinoline, 1,2-dihydro-2,2,4-trimethyl-. In the third pathway, ketones (e.g. 2-cyclopenten-1-one, 2,3-dimethyl-) and alcohols (e.g. 1-Hexadecanol, 2-methyl-) mostly convert from carbohydrates by hydrolysis, dehydration, and cyclization [107].

Previous GC-MS analyses of oils produced through HTL of various macroalgae, including *Ulva prolifera* [133], *Enteromorpha prolifera* [109], *Gracilaria gracilis*, and *Cladophora glomerata* [134], have shown that biocrude compositions can vary significantly among different algal sources. These oils have been found to contain fatty acids (e.g., C14-C20), long-chain hydrocarbons (e.g., C17-C22), aromatics, and other polar substances such as phenols, alcohols, and nitrogen-containing compounds. While this study also identified similar compounds, including fatty acids and nitrogenous heterocyclic compounds in the biocrude, some constituents differed from those identified in earlier research. These differences in biocrude composition were influenced not only by the type of algal feedstock but also by the conditions under which liquefaction occurred. From GC-MS analysis it can be seen that the content of acids exceeds 56 %, and the N-containing compounds are around 18 %. The specific percentage of nitrogen-containing compounds in biocrude can vary significantly depending on algae species, reaction conditions, and efficiency of nitrogen removal pathways [1]. Studies noted that higher temperatures resulted in a biocrude with a low nitrogen content and an aqueous phase with a high content of nitrogen [132]. Throughout the process, various nitrogen-containing compounds are formed, but many of these compounds are volatile and are removed as gas and aqueous phase [1], leading to reduction in nitrogen content of final biocrude. The HTL deamination involves the removal of amino groups (NH_2) from amino acids and other nitrogen-containing compounds. While decarboxylation primarily involves the removal of carbon dioxide, it can also result in the removal of nitrogen, particularly when it occurs in conjunction with deamination [1,135]. The removed nitrogen is typically released as ammonia or other nitrogen-containing compounds in gas and aqueous phase [1,77]. Also, the Maillard reactions can occur between amino acids and reducing sugars, leading to the formation of volatile nitrogen-containing compounds in gas and aqueous phase [132]. Additional refinement processes, including the removal of oxygen (deoxygenation) and nitrogen (denitrogenation), are imperative to render biocrude compatible for use as an engine fuel [136]. These enhancements are crucial to meet the stringent specifications for fuel properties and performance characteristics required for efficient combustion in engines.

Table 9
Boiling point distribution of biocrude obtained from the optimum condition.

Distillate range (°C)	Typical application	Biocrude (%)
25–110	Bottle gas and chemicals	3.71
110–200	Gasoline	17.22
200–300	Jet fuel, fuel for stoves, and diesel oil	35.79
300–400	Lubricating oil for engines, fuel for ships, and machines	28.03
400–550	Lubricants and candles, fuel for ships	12.15
550–700	Fuel for ships, factories, and central heating	1.42
700–800	Asphalt and roofing	0.84
>800	Residues	0.84

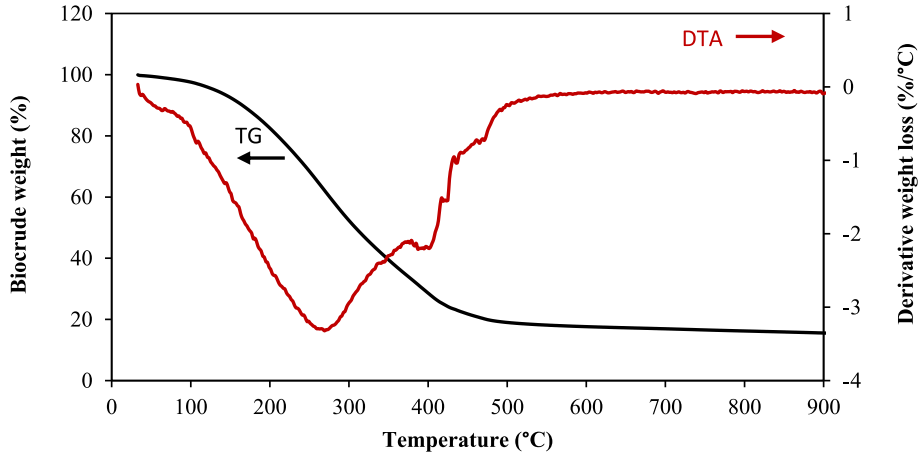

Fig. 6. TG (black line) and DTA (red line) curves of biocrude. (For interpretation of the references to colour in this figure legend, the reader is referred to the Web version of this article.)

3.3.4. TGA analysis

TGA applied in simulated distillation is regarded as miniature distillation and provides an estimate of the boiling range of biocrude. Thermogravimetry (TG)/differential thermal analysis (DTG) curves of biocrude are presented in Fig. 6. Biocrude heating under an inert atmosphere to 900 °C resulted in about 85 % weight loss. The weight loss of biocrude before 110 °C was 3.14 %, which indicates the drying process effectively removed the DCM solvent. The most weight loss for biocrude occurring below 400 °C was 84.75 %. Overall, TG/TGA characterizations of biocrude showed that biocrude contained large distillable fractions. Table 9 presents the boiling point distribution of biocrude. The distribution of petroleum products at different temperatures was adopted from the literature [137,138]. The main biocrude distribution was mainly in the range of 110–550 °C. Bicrude contained a significant amount of boiling point fractions (63.82 %) at 200–400 °C. Moreover, the fractions at 200–300 °C accounted for the highest biocrude weight loss of 35.79 %, representing the fraction of diesel oil. It is consistent with the previous studies [110,138–140] that, most biocrude fractions were light in the range of jet fuel and diesel. However, the biocrude contained significant amounts of oxygen and nitrogen. Therefore, there is a need for following upgrading stages to enhance biocrude quality. Moreover, the weight loss of biocrude at 300–400 °C was 28.03 %, which was the fraction of lubricant oil for engines and fuel for ships. This result also agrees with the GC–MS result where compounds of the same boiling range, i.e. Hexadecanoic acid and Tetradecanoic acid were found. However, major components of biocrude obtained from cornstalk [111], *Scenedesmus* [68], *Chlorella*, and *Spirulina* microalgae [10] fall in the category of lubricant and fuel for the ship. TGA of biocrude obtained from *Caulerpa sertularioides* macroalgae indicates that the higher biocrude quality is achievable according to the higher amount of low boiling point fractions.

3.4. Solid residue characterization

Solid residue analysis is shown in Table 10. The produced solid from *Caulerpa sertularioides* had 12.50 % carbon, 7.05 % hydrogen, 4.65 % nitrogen, and 24.56 % oxygen at 350 °C. The amount of carbon (12.50 %) had decreased significantly compared to the initial feed (25.93 %). The HHV of solid residue from *Caulerpa sertularioides* was calculated at 8.97 MJ/kg, which was slightly higher than the HHV of HTL solid residue from *Sargassum angustifolium* at 350 °C (5.61 MJ/kg) [49].

The surface properties of macroalgae biochar depend on the production method and the properties of the raw materials. The average pore size, surface area, and total pore volume of the solid phase were obtained by BET analysis. According to the resulting linear isotherm shown in Figs. S24–S25, the surface area was measured at 4.54 m^2/g, which is twice the specific surface area of the macroalgae (2.26 m^2/g). As reported by Leng et al., the biochar obtained from macroalgae typically has a small surface area (1–5 m^2/g) [141]. The low surface area of solid residue may be justified by the fact that it also happened to have a large average particle size, as concluded from the particle size distribution (1.97 and 233.60 nm) [142]. The surface area increases due to the escape of volatile materials produced by macroalgae [79].

Table 10
Analysis of solid phase.

Component/Property	Solid residue	Algal feedstock
C (wt%)	12.50	25.93
H (wt%)	7.05	3.58
N (wt%)	4.65	2.52
O (wt%)	24.56	21.59
Ash (wt%)	51.24	46.39
HHV (MJ/kg)	8.97	10.02
Surface area (m^2/g)	4.54	2.269
Pore volume (cm^3/g)	0.027	0.0043
Pore size (nm)	9.89	3.52

Table 11
Analysis of aqueous phase.

Property	Aqueous phase
COD	14360 mg/l
TOC	6031 mg/l
TDS	1657 mg/l
TN	9550 mg/l
pH	7.91

The solid material produced from *Caulerpa sertularioides* had a pore diameter of 98.97 Å (9.89 nm) and can be classified as mesoporous material (between 2 and 50 nm). Amar et al. observed that the significant pore volume of HTL solid residue was mainly confined to the average pore size of 8–14 nm [143]. Also, the total pore volume of solid residue was 0.027 cm^3/g, which was near to the pore volume of solid co-products of the HTL process of corn stover (0.02–0.03 cm^3/g) [143,144].

3.5. Aqueous phase characterization

The properties of the aqueous phase are presented in Table 11. The chemical oxygen demand was detected at 14360 mg/l, which was near the COD of 19475 mg/l reported for the HTL aqueous phase of sewage sludge at 300 °C for 30 min [145]. The high value of COD indicates the presence of high organic contents that could lead to ecological concerns if this effluent is released without treatment. The amount of TOC found within the liquid phase varies considerably with the biomass utilized, the density of solids within the reaction vessel, and the reaction conditions [146]. The TOC was found 6.031 g/l, which was close to the TOC of 6.171 g/l reported for the aqueous phase from HTL of sludge with a biomass concentration of 10 wt% [147]. The higher protein content of the feedstock and higher content of polar compounds in the HTL liquid phase lead the higher TOC in the aqueous phase [64]. The cultivation of algae utilizing dissolved organic carbon in water presents an economically and technologically viable approach [148]. The TN was obtained at 9550 mg/l, corresponding to the high nitrogen content of the aqueous phase. The TN of the HTL aqueous phase of *Caulerpa sertularioides* was higher than *Nannochloropsis gaditana* (5419 mg/l) and *Scenedesmus almeriensis* (4039 mg/l) at 350 °C [149], because algae containing high proteins give higher TNs [74]. Many studies indicated that the nitrogen in the aqueous phase is in NH_4^+ form [74,150,151]. Elevated concentrations of ammonium within the aquatic phase indicate a promising opportunity for nitrogen recuperation through the proliferation of algae. This is attributed to the fact that algae can assimilate ammonium with greater efficiency for the biosynthesis of nitrogenous cellular compounds as compared to utilizing nitrate [74]. The TDS and pH were detected at 1657 mg/l and 7.91, respectively. The pH of the aqueous phase was slightly alkaline, which was supported by pH (typically ~8) reported for the HTL aqueous phase of different microalgae and macroalgae [64]. The presence of ammonia in the water-based component is attributable to the breakdown of proteins within the algal cells. Consequently, a greater concentration of proteins in the initial biomass correlates with an elevated pH level in the HTL aqueous phase. Also, algae can grow rapidly in slightly alkaline environments. Therefore, the pH value of 7.91 shows the potential of the aqueous product for algae cultivation. However, relatively high amounts of COD and TDS make it necessary to dilute this phase before using it as an algae culture medium.

3.6. Gas phase characterization

The gas chromatography indicated that the gas phase contained 79.46 % CO_2, 1.52 % H_2, 1.20 % N_2, 0.46 % C_2H_6, 0.39 % CH_4, and 11.81 % others. Results indicated that CO_2 is typically present in the highest amount, which is common for HTL of biomass [152]. CO_2 could be formed from reactions such as water-gas shift reaction, steam

Table 12
Pretreatment HTL of *Caulerpa sertularioides*.

Experiment	Condition	Y_{SR} (wt%)	Y_{AP} (wt%)	Y_{BC} (wt%)	Y_G (wt %)
Conventional HTL	HTL: 350 °C, 8.6 wt% for 35min	22.62	42.25	10.34	24.79
Ultrasonic + HTL	Pretreatment: Power = 50W for 1min	15.38	53.05	9.53	22.04
Ultrasonic + HTL	Pretreatment: Power = 50W for 15min	17.44	45.34	8.52	28.7
Ultrasonic + HTL	Pretreatment: Power = 75W for 1min	16.74	55.68	6.74	20.84
Ultrasonic + HTL	Pretreatment: Power = 75W for 15min	10.46	44.52	4.84	40.18
Ultrasonic + HTL	Pretreatment: Power = 134W for 15min	13.93	50.57	5.93	29.57
Microwave + HTL	Pretreatment: Power = 500W for 1min	14.33	75.13	7.44	3.10
Microwave + HTL	Pretreatment: Power = 600W for 1min	16.69	70.86	8.64	3.81

reforming, and decarboxylation [66,153]. However, the low amount of H_2 to CO_2 ratio and differences in activation energies for their formation during HTL (38 ± 3 kJ/mol vs. 99 ± 5 kJ/mol, respectively) indicate that decarboxylation is most likely to occur [153]. Moreover, the gas formation is thought to mainly arise from radical reactions, but the high protein content of the feedstock means that a large number of free radical scavengers are formed which includes N-containing heterocyclic aromatic organic compounds [154].

3.7. Pretreatment of HTL

The microwave and ultrasonic pretreatments were performed at 350 °C, 130 bar, and 8.6 wt% feed concentration. Comparison was made between conventional HTL and the HTL assisted by microwave and ultrasonic pretreatment and results are shown in Table 12. The solid yield decreased with the increase of ultrasonic and microwave power, indicating an increase in biomass biodegradation. However, biomass biodegradation was in favor of the aqueous phase and had a negative impact on the yield of biocrude. When the power increased from ultrasonic to microwave, the aqueous phase yield increased significantly. Moreover, biocrude yield decreased with the increase in ultrasonic pretreatment time from 1 min to 15 min. By increasing microwave power from 500 to 600 W, the aqueous phase converted to the biocrude and gas phase, and the biocrude and gas yields increased slightly to 8.64 wt% and 3.81 wt%. Higher biocrude yields were obtained at conventional HTL of *Caulerpa sertularioides* without pretreatment as well as the lowest pretreatment power and time. It is expected to be due to high protein and low lipid content in algae. This result was confirmed by Hu et al. [39] and Shi et al. [155], who carried out HTL with ultrasonic pretreatment. They showed that in comparison with conventional HTL, the lower bio-oil yield was achieved in ultrasonication pretreatment. Compared to high-power ultrasonication (75 & 134 W), the yield of bio-oil had higher values in the microwave-assisted HTL process, but it was still lower than the yield in the conventional HTL. This is because the larger molecules break into smaller molecules in high pretreatment power via decomposition and re-polymerization [155].

The pretreatment effect on biocrude yields obtained from untreated and treated algae at 350 °C is in agreement with previous studies. For instance, Eboibi et al. [156] discovered that the HTL of microalgae biomass that had undergone pretreatment resulted in reduced biocrude production compared to yields from raw, unprocessed microalgae. Similarly, Zou et al. [81] observed a decrease in biocrude yield by approximately 10 wt% when processing *D. tertiolecta*. that had been subjected to pretreatment compared to processing of untreated *D. tertiolecta* [81]. Furthermore, Vardon et al. [68] noted a biocrude yield of 31 wt% from defatted *Scenedesmus* sp., which was significantly lower than the yield (45 wt%) achieved from *Scenedesmus* sp. without lipid extraction [156]. Compared to processing of untreated *D. tertiolecta* [81]. The study of Biller et al. [48] showed that the microwave pretreatment of *Nannochloropsis* and *C. fritschii* before HTL did not appear to be particularly beneficial due to reduced biocrude yield. In general, it can be concluded that the pretreatment is not effective on *Caulerpa sertularioides* algae to increase biocrude production in these conditions.

4. Directions for future work

There are some significant opportunities and challenges associated with the large-scale application of algae for biofuel production that need to be addressed in future research. Many macroalgae species are found, but few samples were examined for biofuel production. Further research is necessary to compare performance and find the best feedstock before establishing a biorefinery in coastal areas. Also, understanding the interaction between HTL parameters needs a detailed study to find their impact on the use of HTL product yields. Moreover, characteristics of the algal cell wall must be considered in the selection of pretreatment technique, energy demand, and process design to improve product recovery and extraction. In addition, extensive research is required to achieve a deep understanding of the relationship between cell wall characteristics and disruption efficiency. Moreover, the quality of biocrude obtained from HTL is lower than that from petroleum-based fuels. Therefore, the produced biofuel needs upgrading to meet the fuel standards. A variety of techniques have been established to enhance the quality of biocrude, including the use of supercritical fluid processing, the application of esterification reactions, the implementation of catalytic cracking procedures, the employment of hydrogenation processes, the practice of hydrodeoxygenation, and the incorporation of emulsification strategies. The selection of an appropriate enhancement method in conjunction with HTL is pivotal in advancing the quality of biocrude.

5. Conclusion

HTL of *Caulerpa sertularioides* was performed at 250–350 °C, 50–150 bar, and 3–10 wt% feed concentration. The RSM with CCD was used to optimize the operating parameters in HTL. Results showed that more biomass decomposes to HTL products with an increase in temperature and pressure. Optimization results indicate that the highest biocrude yield was obtained at 350 °C and 150 bar in 9.752 wt%. In optimal conditions, the yield of biocrude in the experiment was obtained at 22.15 wt%. Furthermore, the biocrude characterization showed that biocrude had a range of 63–74 %, 7–11 %, 2–4.5 %, and 9–25 % for carbon, hydrogen, nitrogen, and oxygen, respectively. Also, HTL of *Caulerpa sertularioides* at 350 °C and 150 bar resulted in a maximum ER of 73.19 %. The maximum HHV of 39.17 MJ/kg was obtained at 300 °C and 184 bar. The FT-IR and GC-MS analysis showed that the main compounds of biocrude were acids, ketones, and heterocyclic compounds. Although the boiling point of 35.79 % of biocrude components was the same as the boiling point of diesel oil (200–300 °C), the biocrude contained high oxygen content. Thus, subsequent deoxygenation steps may make this feasible for fuel production of *Caulerpa sertularioides*. Finally, an investigation of ultrasonic and microwave pretreatment effects suggested that solid and biocrude yields decreased, while the aqueous phase increased with the increase of pretreatment power. It turned out that the pretreatment was not effective in increasing biocrude production from *Caulerpa sertularioides* algae at 350 °C.

CRediT authorship contribution statement

Ziba Borazjani: Investigation. **Reza Azin:** Supervision. **Shahriar Osfouri:** Supervision. **Rahim Karami:** Writing – review & editing. **Eric Kennedy:** Writing – review & editing. **Michael Stockenhuber:** Writing – review & editing.

Declaration of competing interest

The authors declare that they have no competing financial interests or personal relationships that would appear to influence the work reported in this paper.

Acknowledgments

Z. Borazjani expresses gratitude to S.M.R Hashemipour for providing technical assistance. This manuscript was prepared without the support of any financial contributions.

Appendix A. Supplementary data

Supplementary data to this article can be found online at https://doi.org/10.1016/j.biombioe.2025.107635.

Data availability

Data will be made available on request.

References

[1] I.A. Basar, H. Liu, H. Carrere, E. Trably, C. Eskicioglu, A review on key design and operational parameters to optimize and develop hydrothermal liquefaction of biomass for biorefinery applications, Green Chem. 23 (2021) 1404–1446, https://doi.org/10.1039/d0gc04092d.

[2] Z. Borazjani, R. Azin, S. Osfouri, M. Lehner, M. Ellersdorfer, Computer-aided exergy evaluation of hydrothermal liquefaction for biocrude production from Nannochloropsis sp, Bioenergy Res 15 (2022) 141–153, https://doi.org/10.1007/s12155-021-10297-x.

[3] Y. Xue, H. Chen, W. Zhao, C. Yang, P. Ma, S. Han, A review on the operating conditions of producing bio-oil from hydrothermal liquefaction of biomass, Int. J. Energy Res. 40 (2016) 865–877, https://doi.org/10.1002/er.3473.

[4] B.E. Eboibi, Impact of time on yield and properties of biocrude during downstream processing of product mixture derived from hydrothermal liquefaction of microalga, Biomass Convers. Biorefinery 9 (2019) 379–387, https://doi.org/10.1007/s13399-019-00371-y.

[5] P. Ranganathan, S. Savithri, Techno-economic analysis of microalgae-based liquid fuels production from wastewater via hydrothermal liquefaction and hydroprocessing, Bioresour. Technol. 284 (2019) 256–265, https://doi.org/10.1016/j.biortech.2019.03.087.

[6] J. Zhang, B. Jiang, D. Wang, Thermogravimetric and kinetic analysis of bio-crude from hydrothermal liquefaction of Enteromorpha prolifera, Algal Res. 18 (2016) 45–50, https://doi.org/10.1016/j.algal.2016.06.005.

[7] R.K. Mishra, V. kumar, P. Kumar, K. Mohanty, Hydrothermal liquefaction of biomass for bio-crude production: a review on feedstocks, chemical compositions, operating parameters, reaction kinetics, techno-economic study, and life cycle assessment, Fuel 316 (2022) 123377, https://doi.org/10.1016/J.FUEL.2022.123377.

[8] J. Remón, J. Randall, V.L. Budarin, J.H. Clark, Production of bio-fuels and chemicals by microwave-assisted, catalytic, hydrothermal liquefaction (MAC-HTL) of a mixture of pine and spruce biomass, Green Chem. 21 (2019) 284–299, https://doi.org/10.1039/c8gc03244k.

[9] S.S. Toor, L. Rosendahl, A. Rudolf, Hydrothermal liquefaction of biomass: a review of subcritical water technologies, Energy 36 (2011) 2328–2342, https://doi.org/10.1016/j.energy.2011.03.013.

[10] C. Jazrawi, P. Biller, A.B. Ross, A. Montoya, T. Maschmeyer, B.S. Haynes, Pilot plant testing of continuous hydrothermal liquefaction of microalgae, Algal Res. 2 (2013) 268–277, https://doi.org/10.1016/j.algal.2013.04.006.

[11] Y. Han, S.K. Hoekman, Z. Cui, U. Jena, P. Das, Hydrothermal liquefaction of marine microalgae biomass using co-solvents, Algal Res. 38 (2019) 101421, https://doi.org/10.1016/j.algal.2019.101421.

[12] S. Nagappan, R.R. Bhosale, D.D. Nguyen, N.T.L. Chi, V.K. Ponnusamy, C. S. Woong, G. Kumar, Catalytic hydrothermal liquefaction of biomass into bio-oils and other value-added products–A review, Fuel 285 (2021) 119053, https://doi.org/10.1016/j.fuel.2020.119053.

[13] D. Lachos-Perez, P.C. Torres-Mayanga, E.R. Abaide, G.L. Zabot, F. De Castilhos, Hydrothermal carbonization and Liquefaction: differences, progress, challenges, and opportunities, Bioresour. Technol. 343 (2022) 126084, https://doi.org/10.1016/j.biortech.2021.126084.

[14] B.E.O. Eboibi, D.M. Lewis, P.J. Ashman, S. Chinnasamy, Hydrothermal liquefaction of microalgae for biocrude production: improving the biocrude properties with vacuum distillation, Bioresour. Technol. 174 (2014) 212–221, https://doi.org/10.1016/j.biortech.2014.10.029.

[15] D. Zhou, L. Zhang, S. Zhang, H. Fu, J. Chen, Hydrothermal liquefaction of macroalgae enteromorpha prolifera to bio-oil, Energy Fuel. 24 (2010) 4054–4061, https://doi.org/10.1021/ef100151h.

[16] J. Arun, P. Varshini, P.K. Prithvinath, V. Priyadarshini, K.P. Gopinath, Enrichment of bio-oil after hydrothermal liquefaction (HTL) of microalgae C. vulgaris grown in wastewater: bio-char and post HTL wastewater utilization studies, Bioresour. Technol. 261 (2018) 182–187, https://doi.org/10.1016/j.biortech.2018.04.029.

[17] A.C. Fernandes, B. Biswas, J. Kumar, T. Bhaskar, U.D. Muraleedharan, Valorization of the red macroalga Gracilaria corticata by hydrothermal liquefaction: product yield improvement by optimization of process parameters, Bioresour. Technol. Rep. 15 (2021) 100796, https://doi.org/10.1016/j.biteb.2021.100796.

[18] B.E. Eboibi, D.M. Lewis, P.J. Ashman, S. Chinnasamy, Effect of operating conditions on yield and quality of biocrude during hydrothermal liquefaction of halophytic microalga Tetraselmis sp, Bioresour. Technol. 170 (2014) 20–29, https://doi.org/10.1016/j.biortech.2014.07.083.

[19] C. Xu, J. Lancaster, Conversion of secondary pulp/paper sludge powder to liquid oil products for energy recovery by direct liquefaction in hot-compressed water, Water Res. 42 (2008) 1571–1582, https://doi.org/10.1016/j.watres.2007.11.007.

[20] B. Zhang, M. von Keitz, K. Valentas, Thermochemical liquefaction of high-diversity grassland perennials, J. Anal. Appl. Pyrolysis 84 (2009) 18–24, https://doi.org/10.1016/j.jaap.2008.09.005.

[21] Z. Borazjani, R. Azin, S. Osfouri, Kinetics studies and performance analysis of algae hydrothermal liquefaction process, Biomass Convers. Biorefinery 14 (2023) 19257–19284, https://doi.org/10.1007/s13399-023-04067-2.

[22] Z. Borazjani, F. Bayat Mastalinezhad, R. Azin, S. Osfouri, Global perspective of hydrothermal liquefaction of algae: a review of the process, kinetics, and economics analysis, BioEnergy Res 16 (2023) 1493–1511, https://doi.org/10.1007/s12155-023-10615-5.

[23] C. Yang, S. Wang, J. Yang, D. Xu, Y. Li, J. Li, Y. Zhang, Hydrothermal liquefaction and gasification of biomass and model compounds: a review, Green Chem. 22 (2020) 8210–8232, https://doi.org/10.1039/D0GC02802A.

[24] B. Liu, Z. Wang, L. Feng, Effects of reaction parameter on catalytic hydrothermal liquefaction of microalgae into hydrocarbon rich bio-oil, J. Energy Inst. 94 (2021) 22–28, https://doi.org/10.1016/j.joei.2020.10.008.

[25] Y. Li, C. Zhu, J. Jiang, Z. Yang, W. Feng, L. Li, Y. Guo, J. Hu, Hydrothermal liquefaction of macroalgae with in-situ-hydrogen donor formic acid: effects of process parameters on products yield and characterizations, Ind. Crops Prod. 153 (2020) 112513, https://doi.org/10.1016/j.indcrop.2020.112513.

[26] H.K. Reddy, T. Muppaneni, S. Ponnusamy, N. Sudasinghe, A. Pegallapati, T. Selvaratnam, M. Seger, B. Dungan, N. Nirmalakhandan, T. Schaub, F. O. Holguin, P. Lammers, W. Voorhies, S. Deng, Temperature effect on hydrothermal liquefaction of Nannochloropsis gaditana and Chlorella sp, Appl. Energy 165 (2016) 943–951, https://doi.org/10.1016/j.apenergy.2015.11.067.

[27] Y. Huang, Y. Chen, J. Xie, H. Liu, X. Yin, C. Wu, Bio-oil production from hydrothermal liquefaction of high-protein high-ash microalgae including wild Cyanobacteria sp. and cultivated Bacillariophyta sp, Fuel 183 (2016) 9–19, https://doi.org/10.1016/j.fuel.2016.06.013.

[28] S. Yin, R. Dolan, M. Harris, Z. Tan, Subcritical hydrothermal liquefaction of cattle manure to bio-oil: effects of conversion parameters on bio-oil yield and characterization of bio-oil, Bioresour. Technol. 101 (2010) 3657–3664, https://doi.org/10.1016/j.biortech.2009.12.058.

[29] A.A. Peterson, F. Vogel, R.P. Lachance, M. Fröling, M.J. Antal, J.W. Tester, Thermochemical biofuel production in hydrothermal media: a review of sub- and supercritical water technologies, Energy Environ. Sci. 1 (2008) 32–65, https://doi.org/10.1039/b810100k.

[30] A. Mathanker, D. Pudasainee, A. Kumar, R. Gupta, Hydrothermal liquefaction of lignocellulosic biomass feedstock to produce biofuels: parametric study and products characterization, Fuel 271 (2020) 117534, https://doi.org/10.1016/j.fuel.2020.117534.

[31] L. Qian, S. Wang, P.E. Savage, Hydrothermal liquefaction of sewage sludge under isothermal and fast conditions, Bioresour. Technol. 232 (2017) 27–34, https://doi.org/10.1016/j.biortech.2017.02.017.

[32] K.S. Ocfemia, Y. Zhang, T. Funk, Hydrothermal processing of swine manure to oil using a continuous reactor system: effects of operating parameters on oil yield and quality, Trans. ASABE (Am. Soc. Agric. Biol. Eng.) 49 (2006) 1897–1904, https://doi.org/10.13031/2013.22291.

[33] Y. Hu, M. Gong, S. Feng, C.Charles Xu, A. Bassi, A review of recent developments of pre-treatment technologies and hydrothermal liquefaction of microalgae for bio-crude oil production, Renew. Sustain. Energy Rev. 101 (2019) 476–492, https://doi.org/10.1016/j.rser.2018.11.037.

[34] G. Maffei, M.P. Bracciale, A. Broggi, A. Zuorro, M.L. Santarelli, R. Lavecchia, Effect of an enzymatic treatment with cellulase and mannanase on the structural properties of Nannochloropsis microalgae, Bioresour. Technol. 249 (2018) 592–598, https://doi.org/10.1016/j.biortech.2017.10.062.

[35] Y.A. Ma, Y.M. Cheng, J.W. Huang, J.F. Jen, Y.S. Huang, C.C. Yu, Effects of ultrasonic and microwave pretreatments on lipid extraction of microalgae, Bioproc. Biosyst. Eng. 37 (2014) 1543–1549, https://doi.org/10.1007/s00449-014-1126-4.

[36] J.Y. Park, K. Lee, S.A. Choi, M.J. Jeong, B. Kim, J.S. Lee, Y.K. Oh, Sonication-assisted homogenization system for improved lipid extraction from Chlorella vulgaris, Renew. Energy 79 (2015) 3–8, https://doi.org/10.1016/j.renene.2014.10.001.

[37] T. Garoma, D. Janda, Investigation of the effects of microalgal cell concentration and electroporation, microwave and ultrasonication on lipid extraction efficiency, Renew. Energy 86 (2016) 117–123, https://doi.org/10.1016/j.renene.2015.08.009.

[38] Y.M. Heo, H. Lee, C. Lee, J. Kang, J.W. Ahn, Y.M. Lee, K.Y. Kang, Y.E. Choi, J. J. Kim, An integrative process for obtaining lipids and glucose from Chlorella vulgaris biomass with a single treatment of cell disruption, Algal Res. 27 (2017) 286–294, https://doi.org/10.1016/j.algal.2017.09.022.
[39] Y. Hu, M. Gong, C.Charles Xu, A. Bassi, Investigation of an alternative cell disruption approach for improving hydrothermal liquefaction of microalgae, Fuel 197 (2017) 138–144, https://doi.org/10.1016/j.fuel.2017.02.022.
[40] R. Halim, R. Harun, M.K. Danquah, P.A. Webley, Microalgal cell disruption for biofuel development, Appl. Energy 91 (2012) 116–121, https://doi.org/10.1016/j.apenergy.2011.08.048.
[41] A. Moure Abelenda, A. Study of the Effect of the Ultrasonic Pretreatment on the Hydrothermal Liquefaction of Microalgae, 2016. Cranfield.
[42] B. Zhang, H. Feng, Z. He, S. Wang, H. Chen, Bio-oil production from hydrothermal liquefaction of ultrasonic pre-treated Spirulina platensis, Energy Convers. Manag. 159 (2018) 204–212, https://doi.org/10.1016/j.enconman.2017.12.100.
[43] M. Saber, A. Golzary, H. Wu, F. Takahashi, K. Yoshikawa, Ultrasonic pretreatment for low-temperature hydrothermal liquefaction of microalgae: enhancing the bio-oil yield and heating value, Biomass Convers. Biorefinery 8 (2018) 509–519, https://doi.org/10.1007/s13399-017-0300-8.
[44] K. Kapusta, Effect of ultrasound pretreatment of municipal sewage sludge on characteristics of bio-oil from hydrothermal liquefaction process, Waste Manag. 78 (2018) 183–190, https://doi.org/10.1016/j.wasman.2018.05.043.
[45] M.T.H. Siddiqui, F.L. Chan, S. Nizamuddin, H.A. Baloch, S. Kundu, M. Czajka, G. J. Griffin, A. Tanksale, K. Shah, M. Srinivasan, Comparative study of microwave and conventional solvothermal synthesis for magnetic carbon nanocomposites and bio-oil from rice husk, J. Environ. Chem. Eng. 7 (2019) 103266, https://doi.org/10.1016/j.jece.2019.103266.
[46] J.Y. Lee, C. Yoo, S.Y. Jun, C.Y. Ahn, H.M. Oh, Comparison of several methods for effective lipid extraction from microalgae, Bioresour. Technol. 1 (2010) S75–S77, https://doi.org/10.1016/j.biortech.2009.03.058.
[47] C. Onumaegbu, A. Alaswad, C. Rodriguez, A. Olabi, Modelling and optimization of wet microalgae Scenedesmus quadricauda lipid extraction using microwave pre-treatment method and response surface methodology, Renew. Energy 132 (2019) 1323–1331, https://doi.org/10.1016/j.renene.2018.09.008.
[48] P. Biller, C. Friedman, A.B. Ross, Hydrothermal microwave processing of microalgae as a pre-treatment and extraction technique for bio-fuels and bio-products, Bioresour. Technol. 136 (2013) 188–195, https://doi.org/10.1016/j.biortech.2013.02.088.
[49] F.B. Mastalinezhad, S. Osfouri, R. Azin, Production and characterization of biocrude from Persian Gulf Sargassum angustifolium using hydrothermal liquefaction: process optimization by response surface methodology, Biomass Bioenergy 178 (2023) 106963, https://doi.org/10.1016/j.biombioe.2023.106963.
[50] D.L. Barreiro, M. Beck, U. Hornung, F. Ronsse, A. Kruse, W. Prins, Suitability of hydrothermal liquefaction as a conversion route to produce biofuels from macroalgae, Algal Res. 11 (2015) 234–241, https://doi.org/10.1016/j.algal.2015.06.023.
[51] A. Aslani, M. Mohammadi, M.J.I. Gonzalez, T.M. Sobczuk, M. Nazari, A. Bakhtiar, Evaluation of the potentials and feasibility of microalgae production in Iran, Bioresour. Technol. Rep. 1 (2018) 24–30, https://doi.org/10.1016/j.biteb.2017.12.001.
[52] R. Villares, A. Carballeira, Seasonal variation in the concentrations of nutrients in two green macroalgae and nutrient levels in sediments in the Rías Baixas (NW Spain), Estuar. Coast Shelf Sci. 58 (2003) 887–900, https://doi.org/10.1016/j.ecss.2003.07.004.
[53] H.M. Khairy, S.M. El-Shafay, Seasonal variations in the biochemical composition of some common seaweed species from the coast of Abu Qir Bay, Alexandria, Egypt, Oceanologia 55 (2013) 435–452, https://doi.org/10.5697/oc.55-2.435.
[54] Y. Moustafa, S. Saeed, Nutritional evaluation of green macroalgae, Ulva sp. and related water nutrients in the Southern Mediterranean Sea coast, Alexandria shore, Egypt, Egypt, Acad. J. Biol. Sci. H. Bot. 5 (2014) 1–19, https://doi.org/10.21608/eajbsh.2014.16825.
[55] T. Nandakumaran, N. Anbalahan, S. Nivetha, S. Arunadevi, P. Revathi, G. Subramanian, Studies on phytochemicals of marine algal species of genus Caulerpa from gulf of Mannar, costal regions, India, World J. Harmaceutical Res. 8 (2019) 1731–1741.
[56] P. Kumari, A.J. Bijo, V.A. Mantri, C.R.K. Reddy, B. Jha, Fatty acid profiling of tropical marine macroalgae: an analysis from chemotaxonomic and nutritional perspectives, Phytochemistry 86 (2013) 44–56, https://doi.org/10.1016/j.phytochem.2012.10.015.
[57] K. Pirian, Z.Z. Jeliani, M. Arman, J. Sohrabipour, M. Yousefzadi, Proximate analysis of selected macroalgal species from the Persian gulf as a nutritional resource, Trop. Life Sci. Res. 31 (2020) 1–17, https://doi.org/10.21315/tlsr2020.31.1.1.
[58] I. Osuna-Ruiz, M. Nieves-Soto, M.M. Manzano-Sarabia, E. Hernández-Garibay, J. Lizardi-Mendoza, A. Burgos-Hernández, M.Á. Hurtado-Oliva, Gross chemical composition, fatty acids, sterols, and pigments in tropical seaweed species off Sinaloa, Cienc. Mar. 45 (2019) 101–120. Mexico.
[59] R. Jayasankar, J.R. Ramalingam, N. Kaliaperumal, Biochemical composition of some green algae from Mandapam coast, Seaweed Res. Util. 12 (1 & 2) (1990) 37–40.
[60] K. Prapaiwatcharapan, S. Sunphorka, P. Kuchonthara, K. Kangvansaichol, N. Hinchiranan, Single- and two-step hydrothermal liquefaction of microalgae in a semi-continuous reactor: effect of the operating parameters, Bioresour. Technol. 191 (2015) 426–432, https://doi.org/10.1016/j.biortech.2015.04.027.
[61] K.P.R. Dandamudi, T. Muppaneni, J.S. Markovski, P. Lammers, S. Deng, Hydrothermal liquefaction of green microalga Kirchneriella sp. under sub- and super-critical water conditions, Biomass Bioenergy 120 (2019) 224–228, https://doi.org/10.1016/j.biombioe.2018.11.021.
[62] Z. Zhu, L. Rosendahl, S.S. Toor, G. Chen, Optimizing the conditions for hydrothermal liquefaction of barley straw for bio-crude oil production using response surface methodology, Sci. Total Environ. 630 (2018) 560–569, https://doi.org/10.1016/j.scitotenv.2018.02.194.
[63] S. Kandasamy, B. Zhang, Z. He, H. Chen, H. Feng, Q. Wang, B. Wang, N. Bhuvanendran, S. Esakkimuthu, V. Ashokkumar, M. Krishnamoorthi, Hydrothermal liquefaction of microalgae using Fe3O4 nanostructures as efficient catalyst for the production of bio-oil: optimization of reaction parameters by response surface methodology, Biomass Bioenergy 131 (2019) 105417, https://doi.org/10.1016/j.biombioe.2019.105417.
[64] P.G. Duan, S.K. Yang, Y.P. Xu, F. Wang, D. Zhao, Y.J. Weng, X.L. Shi, Integration of hydrothermal liquefaction and supercritical water gasification for improvement of energy recovery from algal biomass, Energy 155 (2018) 734–745, https://doi.org/10.1016/j.energy.2018.05.044.
[65] Y. Gao, H.P. Chen, J. Wang, T. Shi, H.P. Yang, X.H. Wang, Characterization of products from hydrothermal liquefaction and carbonation of biomass model compounds and real biomass, Ranliao Huaxue Xuebao/Journal Fuel Chem. Technol. 39 (2011) 893–900, https://doi.org/10.1016/s1872-5813(12)60001-2.
[66] T.M. Brown, P. Duan, P.E. Savage, Hydrothermal liquefaction and gasification of Nannochloropsis sp, Energy Fuel. 24 (2010) 3639–3646, https://doi.org/10.1021/ef100203u.
[67] W. Yang, X. Li, Z. Li, C. Tong, L. Feng, Understanding low-lipid algae hydrothermal liquefaction characteristics and pathways through hydrothermal liquefaction of algal major components: crude polysaccharides, crude proteins and their binary mixtures, Bioresour. Technol. 196 (2015) 99–108, https://doi.org/10.1016/j.biortech.2015.07.020.
[68] D.R. Vardon, B.K. Sharma, G.V. Blazina, K. Rajagopalan, T.J. Strathmann, Thermochemical conversion of raw and defatted algal biomass via hydrothermal liquefaction and slow pyrolysis, Bioresour. Technol. 109 (2012) 178–187, https://doi.org/10.1016/j.biortech.2012.01.008.
[69] S.A. Channiwala, P.P. Parikh, A unified correlation for estimating HHV of solid, liquid and gaseous fuels, Fuel 81 (2002) 1051–1063, https://doi.org/10.1016/S0016-2361(01)00131-4.
[70] Z. Cui, J.M. Greene, F. Cheng, J.C. Quinn, U. Jena, C.E. Brewer, Co-hydrothermal liquefaction of wastewater-grown algae and crude glycerol: a novel strategy of bio-crude oil-aqueous separation and techno-economic analysis for bio-crude oil recovery and upgrading, Algal Res. 51 (2020) 102077, https://doi.org/10.1016/j.algal.2020.102077.
[71] Y. Xu, K. Liu, Y. Hu, Y. Dong, L. Yao, Experimental investigation and comparison of bio-oil from hybrid microalgae via super/subcritical liquefaction, Fuel 279 (2020) 118412, https://doi.org/10.1016/j.fuel.2020.118412.
[72] N.A.A. Talib, F. Salam, N.A. Yusof, S.A.A. Ahmad, Y. Sulaiman, Optimization of peak current of poly (3, 4-ethylenedioxythiophene)/multi-walled carbon nanotube using response surface methodology/central composite design, RSC Adv. 7 (2017) 11101–11110, https://doi.org/10.1039/C6RA26135C.
[73] S. Leow, J.R. Witter, D.R. Vardon, B.K. Sharma, J.S. Guest, T.J. Strathmann, Prediction of microalgae hydrothermal liquefaction products from feedstock biochemical composition, Green Chem. 17 (2015) 3584–3599, https://doi.org/10.1039/c5gc00574d.
[74] R. Shakya, S. Adhikari, R. Mahadevan, S.R. Shanmugam, H. Nam, E.B. Hassan, T. A. Dempster, Influence of biochemical composition during hydrothermal liquefaction of algae on product yields and fuel properties, Bioresour. Technol. 243 (2017) 1112–1120, https://doi.org/10.1016/j.biortech.2017.07.046.
[75] X. Zhang, K. Wu, Q. Yuan, Comparative study of microwave and conventional hydrothermal treatment of chicken carcasses: bio-oil yields and properties, Energy 200 (2020) 117539, https://doi.org/10.1016/j.energy.2020.117539.
[76] S. Zou, Y. Wu, M. Yang, C. Li, J. Tong, Bio-oil production from sub- and supercritical water liquefaction of microalgae Dunaliella tertiolecta and related properties, Energy Environ. Sci. 3 (2010) 1073–1078, https://doi.org/10.1039/c002550j.
[77] D. López Barreiro, M. Beck, U. Hornung, F. Ronsse, A. Kruse, W. Prins, Suitability of hydrothermal liquefaction as a conversion route to produce biofuels from macroalgae, Algal Res. 11 (2015) 234–241, https://doi.org/10.1016/j.algal.2015.06.023.
[78] S. Raikova, C.D. Le, T.A. Beacham, R.W. Jenkins, M.J. Allen, C.J. Chuck, Towards a marine biorefinery through the hydrothermal liquefaction of macroalgae native to the United Kingdom, Biomass Bioenergy 107 (2017) 244–253, https://doi.org/10.1016/j.biombioe.2017.10.010.
[79] M. Parsa, M. Nourani, M. Baghdadi, M. Hosseinzadeh, M. Pejman, Biochars derived from marine macroalgae as a mesoporous by-product of hydrothermal liquefaction process: characterization and application in wastewater treatment, J. Water Process Eng. 32 (2019) 100942, https://doi.org/10.1016/j.jwpe.2019.100942.
[80] D. Li, L. Chen, D. Xu, X. Zhang, N. Ye, F. Chen, S. Chen, Preparation and characteristics of bio-oil from the marine brown alga Sargassum patens C. Agardh, Bioresour. Technol. 104 (2012) 737–742, https://doi.org/10.1016/j.biortech.2011.11.011.
[81] Z. Shuping, W. Yulong, Y. Mingde, I. Kaleem, L. Chun, J. Tong, Production and characterization of bio-oil from hydrothermal liquefaction of microalgae Dunaliella tertiolecta cake, Energy 35 (2010) 5406–5411, https://doi.org/10.1016/j.energy.2010.07.013.

[82] G. Chen, M. Hu, G. Du, S. Tian, Z. He, B. Liu, W. Ma, Hydrothermal liquefaction of sewage sludge by microwave pretreatment, Energy Fuel. 34 (2020) 1145–1152, https://doi.org/10.1021/acs.energyfuels.9b02155.
[83] R. Halim, T.W.T. Rupasinghe, D.L. Tull, P.A. Webley, Mechanical cell disruption for lipid extraction from microalgal biomass, Bioresour. Technol. 140 (2013) 53–63, https://doi.org/10.1016/j.biortech.2013.04.067.
[84] T.V. Ramachandra, D. Hebbale, Bioethanol from macroalgae: prospects and challenges, Renew. Sustain. Energy Rev. 117 (2020) 109479, https://doi.org/10.1016/j.rser.2019.109479.
[85] M. Mohammadi, H. Tajik, P. Hajeb, Nutritional composition of seaweeds from the northern Persian gulf, Iran. J. Fish. Sci. 12 (2013) 232–240.
[86] A.M. Miranda, D. Ocampo, G.J. Vargas, L.A. Ríos, A.A. Sáez, Nitrogen content reduction on scenedesmus obliquus biomass used to produce biocrude by hydrothermal liquefaction, Fuel 305 (2021) 121592, https://doi.org/10.1016/j.fuel.2021.121592.
[87] Y.B. Seo, Y.W. Lee, C.H. Lee, M.W. Lee, Optical properties of red algae fibers, Ind. Eng. Chem. Res. 49 (2010) 9830–9833, https://doi.org/10.1021/ie101194g.
[88] Y. He, X. Liang, C. Jazrawi, A. Montoya, A. Yuen, A.J. Cole, N. Neveux, N.A. Paul, R. de Nys, T. Maschmeyer, B.S. Haynes, Continuous hydrothermal liquefaction of macroalgae in the presence of organic co-solvents, Algal Res. 17 (2016) 185–195, https://doi.org/10.1016/j.algal.2016.05.010.
[89] K.S. Ocfemia, Y. Zhang, T. Funk, Hydrothermal processing of swine manure to oil using a continuous reactor system: effects of operating parameters on oil yield and quality, Trans. ASABE (Am. Soc. Agric. Biol. Eng.) 49 (2006) 1897–1904, https://doi.org/10.13031/2013.22291.
[90] S. Kumar, Hydrothermal processing of biomass for biofuels, Biofuel Res. J. 1 (2014) 43.
[91] L. Nazari, Z. Yuan, M.B. Ray, C.Charles Xu, Co-conversion of waste activated sludge and sawdust through hydrothermal liquefaction: optimization of reaction parameters using response surface methodology, Appl. Energy 203 (2017) 1–10, https://doi.org/10.1016/j.apenergy.2017.06.009.
[92] X. Wei, D. Jie, Optimization to hydrothermal liquefaction of low lipid content microalgae Spirulina sp. using response surface methodology, J. Chem. 2018 (2018) 2041812, https://doi.org/10.1155/2018/2041812.
[93] Y.H. Chan, A.T. Quitain, S. Yusup, Y. Uemura, M. Sasaki, T. Kida, Optimization of hydrothermal liquefaction of palm kernel shell and consideration of supercritical carbon dioxide mediation effect, J. Supercrit. Fluids 133 (2018) 640–646, https://doi.org/10.1016/j.supflu.2017.06.007.
[94] M.A. Nazem, O. Tavakoli, Bio-oil production from refinery oily sludge using hydrothermal liquefaction technology, J. Supercrit. Fluids 127 (2017) 33–40, https://doi.org/10.1016/j.supflu.2017.03.020.
[95] J. Ni, L. Qian, Y. Wang, B. Zhang, H. Gu, Y. Hu, Q. Wang, A review on fast hydrothermal liquefaction of biomass, Fuel 327 (2022) 125135, https://doi.org/10.1016/j.fuel.2022.125135.
[96] D. Castello, L. Fiori, Supercritical water gasification of biomass: thermodynamic constraints, Bioresour. Technol. 102 (2011) 7574–7582, https://doi.org/10.1016/j.biortech.2011.05.017.
[97] P.J. Valdez, M.C. Nelson, H.Y. Wang, X.N. Lin, P.E. Savage, Hydrothermal liquefaction of Nannochloropsis sp.: systematic study of process variables and analysis of the product fractions, Biomass Bioenergy 46 (2012) 317–331, https://doi.org/10.1016/j.biombioe.2012.08.009.
[98] Y. Qu, X. Wei, C. Zhong, Experimental study on the direct liquefaction of Cunninghamia lanceolata in water, Energy 28 (2003) 597–606, https://doi.org/10.1016/S0360-5442(02)00178-0.
[99] U. Jena, K.C. Das, J.R. Kastner, Effect of operating conditions of thermochemical liquefaction on biocrude production from Spirulina platensis, Bioresour. Technol. 102 (2011) 6221–6229, https://doi.org/10.1016/j.biortech.2011.02.057.
[100] K. Anastasakis, A.B. Ross, Hydrothermal liquefaction of the brown macro-alga Laminaria Saccharina: effect of reaction conditions on product distribution and composition, Bioresour. Technol. 102 (2011) 4876–4883, https://doi.org/10.1016/j.biortech.2011.01.031.
[101] Q.V. Bach, M.V. Sillero, K.Q. Tran, J. Skjermo, Fast hydrothermal liquefaction of a Norwegian macro-alga: screening tests, Algal Res. 6 (2014) 271–276, https://doi.org/10.1016/j.algal.2014.05.009.
[102] P. Biller, A.B. Ross, Potential yields and properties of oil from the hydrothermal liquefaction of microalgae with different biochemical content, Bioresour. Technol. 102 (2011) 215–225, https://doi.org/10.1016/j.biortech.2010.06.028.
[103] N. Neveux, A.K.L. Yuen, C. Jazrawi, M. Magnusson, B.S. Haynes, A.F. Masters, A. Montoya, N.A. Paul, T. Maschmeyer, R. de Nys, Biocrude yield and productivity from the hydrothermal liquefaction of marine and freshwater green macroalgae, Bioresour. Technol. 155 (2014) 334–341, https://doi.org/10.1016/j.biortech.2013.12.083.
[104] S. Hongthong, H.S. Leese, M.J. Allen, C.J. Chuck, Assessing the conversion of various nylon polymers in the hydrothermal liquefaction of macroalgae, Environ. - MDPI. 8 (2021) 34, https://doi.org/10.3390/ENVIRONMENTS8040034.
[105] J. Nallasivam, P. Francis Prashanth, S. Harisankar, S. Nori, S. Suryanarayan, S. R. Chakravarthy, R. Vinu, Valorization of red macroalgae biomass via hydrothermal liquefaction using homogeneous catalysts, Bioresour. Technol. 346 (2022) 126515, https://doi.org/10.1016/j.biortech.2021.126515.
[106] B. Biswas, A. Arun Kumar, Y. Bisht, R. Singh, J. Kumar, T. Bhaskar, Effects of temperature and solvent on hydrothermal liquefaction of Sargassum tenerrimum algae, Bioresour. Technol. 242 (2017) 344–350, https://doi.org/10.1016/j.biortech.2017.03.045.
[107] L. Yan, Y. Wang, J. Li, Y. Zhang, L. Ma, F. Fu, B. Chen, H. Liu, Hydrothermal liquefaction of Ulva prolifera macroalgae and the influence of base catalysts on products, Bioresour. Technol. 292 (2019) 121286, https://doi.org/10.1016/j.biortech.2019.03.125.
[108] J. Li, G. Wang, C. Gao, X. Lv, Z. Wang, H. Liu, Deoxy-liquefaction of Laminaria japonica to high-quality liquid oil over metal modified ZSM-5 catalysts, Energy Fuel. 27 (2013) 5207–5214, https://doi.org/10.1021/ef4004208.
[109] W. Yang, X. Li, S. Liu, L. Feng, Direct hydrothermal liquefaction of undried macroalgae Enteromorpha prolifera using acid catalysts, Energy Convers. Manag. 87 (2014) 938–945, https://doi.org/10.1016/j.enconman.2014.08.004.
[110] K. Anastasakis, A.B. Ross, Hydrothermal liquefaction of four brown macro-algae commonly found on the UK coasts: an energetic analysis of the process and comparison with bio-chemical conversion methods, Fuel 139 (2015) 546–553, https://doi.org/10.1016/j.fuel.2014.09.006.
[111] Z. Zhu, B. Si, J. Lu, J. Watson, Y. Zhang, Z. Liu, Elemental migration and characterization of products during hydrothermal liquefaction of cornstalk, Bioresour. Technol. 243 (2017) 9–16, https://doi.org/10.1016/j.biortech.2017.06.085.
[112] C. Tian, B. Li, Z. Liu, Y. Zhang, H. Lu, Hydrothermal liquefaction for algal biorefinery: a critical review, Renew. Sustain. Energy Rev. 38 (2014) 933–950, https://doi.org/10.1016/j.rser.2014.07.030.
[113] J.G. Speight, The chemistry and technology of petroleum. https://doi.org/10.1201/b16559, 2014.
[114] J. Akhtar, N.A.S. Amin, A review on process conditions for optimum bio-oil yield in hydrothermal liquefaction of biomass, Renew. Sustain. Energy Rev. 15 (2011) 1615–1624, https://doi.org/10.1016/j.rser.2010.11.054.
[115] B. Biswas, A. Kumar, A.C. Fernandes, K. Saini, S. Negi, U.D. Muraleedharan, T. Bhaskar, Solid base catalytic hydrothermal liquefaction of macroalgae: effects of process parameter on product yield and characterization, Bioresour. Technol. 307 (2020) 123232, https://doi.org/10.1016/j.biortech.2020.123232.
[116] N. Sudasinghe, H. Reddy, N. Csakan, S. Deng, P. Lammers, T. Schaub, Temperature-dependent lipid conversion and nonlipid composition of microalgal hydrothermal liquefaction oils monitored by fourier transform ion cyclotron resonance mass spectrometry, Bioenergy Res 8 (2015) 1962–1972, https://doi.org/10.1007/s12155-015-9635-9.
[117] F. Cheng, Z. Cui, K. Mallick, N. Nirmalakhandan, C.E. Brewer, Hydrothermal liquefaction of high- and low-lipid algae: mass and energy balances, Bioresour. Technol. 258 (2018) 158–167, https://doi.org/10.1016/j.biortech.2018.02.100.
[118] X. Tang, C. Zhang, Z. Li, X. Yang, Element and chemical compounds transfer in bio-crude from hydrothermal liquefaction of microalgae, Bioresour. Technol. 202 (2016) 8–14, https://doi.org/10.1016/j.biortech.2015.11.076.
[119] J. Chen, Bio-oil production from hydrothermal liquefaction of Pteris vittata L.: effects of operating temperatures and energy recovery, Bioresour. Technol. 265 (2018) 320–327, https://doi.org/10.1016/j.biortech.2018.06.019.
[120] F. Cheng, K. Mallick, S.M. Henkanatte Gedara, J.M. Jarvis, T. Schaub, U. Jena, N. Nirmalakhandan, C.E. Brewer, Hydrothermal liquefaction of Galdieria sulphuraria grown on municipal wastewater, Bioresour. Technol. 292 (2019) 121884, https://doi.org/10.1016/j.biortech.2019.121884.
[121] J. Watson, J. Lu, R. de Souza, B. Si, Y. Zhang, Z. Liu, Effects of the extraction solvents in hydrothermal liquefaction processes: biocrude oil quality and energy conversion efficiency, Energy 167 (2019) 189–197, https://doi.org/10.1016/j.energy.2018.11.003.
[122] F.B. Mastalinezhad, S. Osfouri, R. Azin, Comparison of biocrude production and characterization from Persian Gulf Sargassum angustifolium macroalgae, Chlorella vulgaris, and Spirulina sp. microalgae using hydrothermal liquefaction (HTL): potential of solid residue for heavy metal adsorption, Environ. Sci. Pollut. Res. (2024) 1–14, https://doi.org/10.1007/s11356-024-35542-6.
[123] M.Y. Ong, S. Nomanbhay, Optimization study on microwave-assisted hydrothermal liquefaction of Malaysian macroalgae chaetomorpha sp. for phenolic-rich bio-oil production, Energies 15 (2022) 3974, https://doi.org/10.3390/en15113974.
[124] L.M. Díaz-Vázquez, A. Rojas-Pérez, M. Fuentes-Caraballo, I. V Robles, U. Jena, K. C. Das, Demineralization of Sargassum spp. macroalgae biomass: selective hydrothermal liquefaction process for bio-oil production, Front. Energy Res. 3 (2015) 6, https://doi.org/10.3389/fenrg.2015.00006.
[125] B. Biswas, A.C. Fernandes, J. Kumar, U.D. Muraleedharan, T. Bhaskar, Valorization of Sargassum tenerrimum: value addition using hydrothermal liquefaction, Fuel 222 (2018) 394–401, https://doi.org/10.1016/j.fuel.2018.02.153.
[126] C. Ma, J. Geng, D. Zhang, X. Ning, Hydrothermal liquefaction of macroalgae: influence of zeolites based catalyst on products, J. Energy Inst. 93 (2020) 581–590, https://doi.org/10.1016/j.joei.2019.06.007.
[127] C. Yuan, S. Wang, B. Cao, Y. Hu, A.E.F. Abomohra, Q. Wang, L. Qian, L. Liu, X. Liu, Z. He, C. Sun, Y. Feng, B. Zhang, Optimization of hydrothermal co-liquefaction of seaweeds with lignocellulosic biomass: merging 2nd and 3rd generation feedstocks for enhanced bio-oil production, Energy 173 (2019) 413–422, https://doi.org/10.1016/j.energy.2019.02.091.
[128] A.R.K. Gollakota, N. Kishore, S. Gu, A review on hydrothermal liquefaction of biomass, Renew. Sustain. Energy Rev. 81 (2018) 1378–1392, https://doi.org/10.1016/j.rser.2017.05.178.
[129] A. Dimitriadis, S. Bezergianni, Hydrothermal liquefaction of various biomass and waste feedstocks for biocrude production: a state of the art review, Renew. Sustain. Energy Rev. 68 (2017) 113–125, https://doi.org/10.1016/j.rser.2016.09.120.
[130] C.D. Venkatachalam, S. Sekar, S.R. Ravichandran, M. Sengottian, K.C. Sukumar, D. Chenniappan, G.A. Ramachandran, A review on bio-crude production from algal biomass using catalytic hydrothermal liquefaction process, Environ. Eng. Res. 28 (2023), https://doi.org/10.4491/eer.2022.211.

[131] A. Kruse, N. Dahmen, Hydrothermal biomass conversion: quo vadis? J. Supercrit. Fluids 134 (2018) 114–123, https://doi.org/10.1016/j.supflu.2017.12.035.
[132] J. Watson, T. Wang, B. Si, W.T. Chen, A. Aierzhati, Y. Zhang, Valorization of hydrothermal liquefaction aqueous phase: pathways towards commercial viability, Prog. Energy Combust. Sci. 77 (2020) 100819, https://doi.org/10.1016/j.pecs.2019.100819.
[133] C. Ma, J. Geng, D. Zhang, X. Ning, Hydrothermal liquefaction of macroalgae: influence of zeolites based catalyst on products, J. Energy Inst. 93 (2020) 581–590, https://doi.org/10.1016/j.joei.2019.06.007.
[134] M. Parsa, H. Jalilzadeh, M. Pazoki, R. Ghasemzadeh, M. Abduli, Hydrothermal liquefaction of Gracilaria gracilis and Cladophora glomerata macro-algae for biocrude production, Bioresour. Technol. 250 (2018) 26–34, https://doi.org/10.1016/j.biortech.2017.10.059.
[135] C. Gai, Y. Zhang, W.-T. Chen, P. Zhang, Y. Dong, An investigation of reaction pathways of hydrothermal liquefaction using Chlorella pyrenoidosa and Spirulina platensis, Energy Convers. Manag. 96 (2015) 330–339, https://doi.org/10.1016/j.enconman.2015.02.056.
[136] C. Tian, Z. Liu, Y. Zhang, Hydrothermal liquefaction (HTL): a promising pathway for biorefinery of algae. Algal Biofuels Recent Adv, Futur. Prospect., 2017, pp. 361–391, https://doi.org/10.1007/978-3-319-51010-1_18.
[137] J.G. Speight, Handbook of Petroleum Product Analysis, second ed., 2015, https://doi.org/10.1002/9781118986370.
[138] W.T. Chen, Y. Zhang, J. Zhang, L. Schideman, G. Yu, P. Zhang, M. Minarick, Co-liquefaction of swine manure and mixed-culture algal biomass from a wastewater treatment system to produce bio-crude oil, Appl. Energy 128 (2014) 209–216, https://doi.org/10.1016/j.apenergy.2014.04.068.
[139] S. Yin, N. Zhang, C. Tian, W. Yi, Q. Yuan, P. Fu, Y. Zhang, Z. Li, Effect of accumulative recycling of aqueous phase on the properties of hydrothermal degradation of dry biomass and bio-crude oil formation, Energies 14 (2021) 285, https://doi.org/10.3390/en14020285.
[140] J. Xu, X. Dong, Y. Wang, Hydrothermal liquefaction of macroalgae over various solids, basic or acidic oxides and metal salt catalyst: products distribution and characterization, Ind. Crops Prod. 151 (2020) 112458, https://doi.org/10.1016/j.indcrop.2020.112458.
[141] L.J. Leng, X.Z. Yuan, H.J. Huang, H. Wang, Z. Bin Wu, L.H. Fu, X. Peng, X. H. Chen, G.M. Zeng, Characterization and application of bio-chars from liquefaction of microalgae, lignocellulosic biomass and sewage sludge, Fuel Process. Technol. 129 (2015) 8–14, https://doi.org/10.1016/j.fuproc.2014.08.016.
[142] R. Chand, V. Babu Borugadda, M. Qiu, A.K. Dalai, Evaluating the potential for bio-fuel upgrading: a comprehensive analysis of bio-crude and bio-residue from hydrothermal liquefaction of agricultural biomass, Appl. Energy 254 (2019) 113679, https://doi.org/10.1016/j.apenergy.2019.113679.
[143] V.S. Amar, J.D. Houck, B. Maddipudi, T.A. Penrod, K.M. Shell, A. Thakkar, A. R. Shende, S. Hernandez, S. Kumar, R.B. Gupta, R.V. Shende, Hydrothermal liquefaction (HTL) processing of unhydrolyzed solids (UHS) for hydrochar and its use for asymmetric supercapacitors with mixed (Mn,Ti)-Perovskite oxides, Renew. Energy 173 (2021) 329–341, https://doi.org/10.1016/j.renene.2021.03.126.
[144] K.M. Shell, D.D. Rodene, V. Amar, A. Thakkar, B. Maddipudi, S. Kumar, R. Shende, R.B. Gupta, Supercapacitor performance of corn stover-derived biocarbon produced from the solid co-products of a hydrothermal liquefaction process, Bioresour. Technol. Rep. 13 (2021) 100625, https://doi.org/10.1016/j.biteb.2021.100625.
[145] L.B. Silva Thomsen, K. Anastasakis, P. Biller, Wet oxidation of aqueous phase from hydrothermal liquefaction of sewage sludge, Water Res. 209 (2022) 117863, https://doi.org/10.1016/j.watres.2021.117863.
[146] R.B. Madsen, P. Biller, M.M. Jensen, J. Becker, B.B. Iversen, M. Glasius, Predicting the chemical composition of aqueous phase from hydrothermal liquefaction of model compounds and biomasses, Energy Fuel. 30 (2016) 10470–10483, https://doi.org/10.1021/acs.energyfuels.6b02007.
[147] Y. Kulikova, S. Klementev, A. Sirotkin, I. Mokrushin, M. Bassyouni, Y. Elhenawy, M.A. El-Hadek, O. Babich, Aqueous phase from hydrothermal liquefaction: composition and toxicity assessment, Water 15 (2023) 1681, https://doi.org/10.3390/w15091681.
[148] C. Gai, Y. Zhang, W.T. Chen, Y. Zhou, L. Schideman, P. Zhang, G. Tommaso, C. T. Kuo, Y. Dong, Characterization of aqueous phase from the hydrothermal liquefaction of Chlorella pyrenoidosa, Bioresour. Technol. 184 (2015) 328–335, https://doi.org/10.1016/j.biortech.2014.10.118.
[149] D. López Barreiro, S. Riede, U. Hornung, A. Kruse, W. Prins, Hydrothermal liquefaction of microalgae: effect on the product yields of the addition of an organic solvent to separate the aqueous phase and the biocrude oil, Algal Res. 12 (2015) 206–212, https://doi.org/10.1016/j.algal.2015.08.025.
[150] V. Kumar, S. Kumar, P.K. Chauhan, M. Verma, V. Bahuguna, H.C. Joshi, W. Ahmad, P. Negi, N. Sharma, B. Ramola, I. Rautela, M. Nanda, M.S. Vlaskin, Low-temperature catalyst based hydrothermal liquefaction of harmful macroalgal blooms, and aqueous phase nutrient recycling by microalgae, Sci. Rep. 9 (2019) 11384, https://doi.org/10.1038/s41598-019-47664-w.
[151] A. Matayeva, P. Biller, Hydrothermal liquefaction aqueous phase treatment and hydrogen production using electro-oxidation, Energy Convers. Manag. 244 (2021) 114462, https://doi.org/10.1016/j.enconman.2021.114462.
[152] R.B. Madsen, P.S. Christensen, K. Houlberg, E. Lappa, A.J. Mørup, M. Klemmer, E. M. Olsen, M.M. Jensen, J. Becker, B.B. Iversen, M. Glasius, Analysis of organic gas phase compounds formed by hydrothermal liquefaction of dried distillers grains with solubles, Bioresour. Technol. 192 (2015) 826–830, https://doi.org/10.1016/j.biortech.2015.05.095.
[153] P. Duan, P.E. Savage, Hydrothermal liquefaction of a microalga with heterogeneous catalysts, Ind. Eng. Chem. Res. 50 (2011) 52–61, https://doi.org/10.1021/ie100758s.
[154] S.R. Villadsen, L. Dithmer, R. Forsberg, J. Becker, A. Rudolf, S.B. Iversen, B. B. Iversen, M. Glasius, Development and application of chemical analysis methods for investigation of bio-oils and aqueous phase from hydrothermal liquefaction of biomass, Energy Fuel. 26 (2012) 6988–6998, https://doi.org/10.1021/ef300954e.
[155] W. Shi, J. Jia, Y. Gao, Y. Zhao, Influence of ultrasonic pretreatment on the yield of bio-oil prepared by thermo-chemical conversion of rice husk in hot-compressed water, Bioresour. Technol. 146 (2013) 355–362, https://doi.org/10.1016/j.biortech.2013.07.094.
[156] B.E. Eboibi, D.M. Lewis, P.J. Ashman, S. Chinnasamy, Influence of process conditions on pretreatment of microalgae for protein extraction and production of biocrude during hydrothermal liquefaction of pretreated Tetraselmis sp, RSC Adv. 5 (2015) 20193–20207, https://doi.org/10.1039/c4ra11662c.